Distribution Agreement

In presenting this thesis or dissertation as a partial fulfillment of the requirements for an advanced degree from Emory University, I hereby grant to Emory University and its agents the non-exclusive license to archive, make accessible, and display my thesis or dissertation in whole or in part in all forms of media, now or hereafter known, including display on the world wide web. I understand that I may select some access restrictions as part of the online submission of this thesis or dissertation. I retain all ownership rights to the copyright of the thesis or dissertation. I also retain the right to use in future works (such as articles or books) all or part of this thesis or dissertation.

Signature:

_____ _____

Kiana Jodeiry Date

Genomic Architecture of Regional Measures of Cortical Thickness

By

Kiana Jodeiry

Master's Thesis

Department of Psychology, Clinical Science

_____

Irwin Waldman, Ph.D. Advisor

_____

Michael Treadway, Ph.D. Committee Member

_____

Daniel D. Dilks, Ph.D. Committee Member

Accepted:

_____

Kimberly Jacob Arriola, Ph.D.
Dean of James T. Laney School of Graduate Studies

_____

Date

Genomic Architecture of Regional Measures of Cortical Thickness

By

Kiana Jodeiry

B.S., Literature, B.S., Brain and Cognitive Science, Massachusetts Institute of Technology, 2019

Advisor: Irwin Waldman, PhD

An abstract of a thesis submitted to the Faculty of the James T. Laney School of Graduate Studies of Emory University in partial fulfillment of the requirements for the degree of Master of Arts in Psychology 2023.

Abstract

The cerebral cortex can be organized into dimensions of brain regions with shared genetic influences on cortical thickness. Such dimensions represent novel cortical phenotypes that can facilitate future genomic investigation into diverse and complex behavioral traits. Understanding the underlying organizational principles of genetic influences on brain structure is a critical step towards a mechanistic model of how specific genes influence brain anatomy and possibly mediate neuropsychiatric risk. The current study models the structure of genetic correlations among regional measures of cortical thickness using Genomic Structural Equation Modeling (Genomic SEM), a recently developed R package that applies the methods of structural equation modeling to genetic covariances. Factor analyses identified eight genomic brain factors that do not conform to traditionally defined brain structure boundaries and relate to a combination of biological and structural principles instead. Such findings highlight the complexity of genetic influences on cortical morphology and set the stage for elucidating the micro and macrostructural bases of complex traits such as personality and psychopathology.

Keywords: neuroimaging, genetics, cortical thickness, brain structure, endophenotype

Genomic Architecture of Regional Measures of Cerebral Cortical Thickness

Kiana Jodeiry

Department of Psychology, Emory University

Author Note

The author has no known conflict of interest to disclose.

Correspondence concerning this article should be addressed to Kiana Jodeiry, Dept. of Psychology, 36 Eagle Row Suite 270, Atlanta, GA, 30322. Email: kiana.jodeiry@emory.edu

Table of Contents

Genomic Architecture of Regional Measures of Cerebral Cortical Thickness

The brain is a plausible biological mechanism through which genes influence the development of complex behavior. As such, intermediate phenotypes along the pathway from genes to behavior, such as variation in brain structure, can facilitate future genomic investigation into diverse traits. Regional measures of cortical thickness (CT) are highly heritable (Winkler et al., 2010), influenced by many genetic variants, and have been reliably associated with important life outcomes (Grasby et al., 2020; Valk et al., 2020). Cerebral CT reflects cytoarchitectural characteristics (e.g., the density and arrangement of neurons) and demonstrates changes over the course of development (Valk et al., 2020). In addition, cerebral CT can be especially sensitive to regional disease-specific effects, including both factors such as neuroinflammation that can increase CT and factors such as excessive synaptic pruning that decrease CT (Valk et al., 2020).

Heritability (h^2) is the proportion of the total variation in a given phenotype within a population that is attributable to genetic variation (Smoller et al., 2019). Winkler et al. (2010) assessed the heritability of cortical thickness in a sample of families collected for genetic studies. Roughly 69% of the variation in average thickness across the cerebral cortex was found to be due to genetic variation in the population ($h^2 = 0.691 \pm 0.119$), and the average heritability of thickness in individual regions was 50% ($\overline{h^2} = 0.501 \pm 0.142$; Winkler et al., 2010). Variability in genes can shape neural structure or activity in regions specialized for emotional or cognitive functions, which in turn should influence the expression of behavioral traits. In support of this proposition, Grasby et al. (2020) found that genetic variants that influence brain structure also shape brain function. Grasby et al. (2020) demonstrated that common genetic variants that influence regional CT also affect various behavioral traits such as general cognitive function, Parkinson's disease, depression, neuroticism, ADHD, and insomnia. As such, CT represents a

particularly promising structural measure for investigating the neural products of genes that play a role in shaping complex behavior. Such investigations take a neurogenetic approach, which aims to better understand associations found between genetic variability, brain, and behavior.

Neuroimaging genetics, a technique based on GWAS of in vivo brain measures, has been a uniquely valuable strategy for illustrating how genetic variants, including those that influence complex behavior, can modulate specific neural processes. The goal of genome-wide association studies (GWAS) is to find regions in the genome where variation affects a phenotype. Single nucleotide polymorphisms (SNPs) are the most frequently occurring genetic variation in the human genome and are important markers in many studies that link sequence variations to phenotypic changes (Kim & Misra, 2007). A SNP is a difference in the nucleotide base present at a particular site in the DNA sequence (i.e., the ‘C allele’ or the ‘T allele’ at a specific locus).

Genotyped samples with neuroimaging data are now large enough to employ genome-wide association studies (GWAS) as a means of identifying specific genetic variants associated with cortical thickness. In an ongoing effort to identify genetic variants that affect brain structure, the Enhancing Neuroimaging Genetics through Meta-Analysis (ENIGMA) Consortium recently conducted genome-wide association meta-analyses of regional measures of cortical thickness across 50 cohorts (Thompson et al., 2019). Genome-wide significant loci associated with regional cortical thickness were located near genes that had been previously implicated in crucial neurodevelopmental processes including cell differentiation, migration, adhesion, myelination, and pruning (Grasby et al., 2020). Analysis of the genetic architecture of cortical thickness has potentially large clinical implications. For example, decreased cortical thickness in schizophrenia is thought to correspond to loss of neuropil (i.e., dendrites, axons, and synapses) in accordance with the synaptic overpruning hypothesis (Spocter et al., 2012). The synaptic

overpruning hypothesis of schizophrenia posits that exaggerated pruning of synapses during adolescence and young adulthood explains the onset of the disorder at that age (Keshavan et al., 2020). Decreased thickness in schizophrenia has been suggested to target specific developmental modules, or communities of cortical areas with similar growth trajectories of cortical thickness (Alexander-Bloch et al., 2014). These modules develop in synchrony during normative adolescence and are likely composed of regions influenced by overlapping sets of genes.

Genetic Correlations Between Brain Regions

While it is theoretically possible that the genetic influences on different brain regions are independent of one another, evidence of such genetic autonomy is limited. Instead, the neurodevelopment of multiple structurally distinct brain regions is mediated by common genetic factors (Schmitt et al., 2007, 2010). Pleiotropy refers to the phenomenon whereby the same genetic variants influence two or more phenotypes, or in this case, influence the thickness of two or more cortical regions. A genetic correlation estimates the degree of overlap between the genetic influences on one trait and the genetic influences on a different trait. Patterns of inter-regional genetic correlations form a complex, heterogeneous network and suggest widespread pleiotropic effects whereby the same genetic variants influence the thickness of multiple cortical regions (Alexander-Bloch et al., 2019). In addition, significant genetic correlations in measures of CT between nearby regions are largely convergent with postmortem correlations in gene expression (Alexander-Bloch et al., 2019; Hawrylycz et al., 2012). One of the goals of neuroimaging genetics is to define brain systems that are modulated by genetic variation, including groups of brain regions with shared genetic influences on CT via pleiotropy.

Prior investigations of patterns of genetic correlations in cortical thickness between brain regions have demonstrated support for a higher-order genetic architecture of cortical thickness.

Chen et al. (2013) aimed to identify the boundaries of cortical divisions that are maximally genetically correlated (i.e., under control of shared genetic influences on cortical thickness). The authors used pair-wise genetic correlations between CT measures from every two points (vertices) on the cerebral cortex to generate genetically based subdivisions, which corresponded closely to meaningful structural and functional regions. Chen and colleagues determined the most appropriate number of clusters to explain patterns in the genetic correlation data was twelve based on maximizing quantitative indices of within-group cohesion and between-group separation. Cohesion reflects how closely related (genetically) the regions in a cluster are and separation determined how distinct or well-separated a cluster is from other clusters (Chen et al., 2013). The twelve identified clusters were largely bilaterally symmetric (left and right hemispheres were mirror images) and spatially contiguous, such that within hemispheres clusters were composed of anatomically adjacent regions. While some cluster boundaries mapped onto traditionally parcellated regions (i.e., Brodmann's areas) or gyral patterns, others did not.

Alexander-Bloch et al. (2019) also investigated the higher-order genetic architecture of regional CT but did not assess the question of brain parcellation directly (i.e., how best to divide the brain into distinct regions). Alexander-Bloch et al. (2019) used graph theoretical techniques to model a matrix of genetic correlations between CT measures in 68 regions defined by the Desikan-Killiany atlas (Desikan et al., 2006). These are the same 34 regions as in the data from ENIGMA Consortium (Grasby et al., 2020) but with contralateral homologs (i.e., the same region represented in each cerebral hemisphere) as separate regions. The authors also found that modules were largely composed of bilaterally symmetric, spatially contiguous regions of the cortical surface. Only five regions had higher genetic correlations with any other region than with their homolog in the opposite hemisphere. Exceptions included canonical language areas

with known functional asymmetry in the inferior prefrontal cortex (e.g., the left bank of the superior temporal sulcus, left pars opercularis and triangularis) as well as the left rostral middle frontal gyrus and right caudal anterior cingulate (Alexander-Bloch et al., 2019).

Unlike Chen et al. (2013), Alexander-Bloch et al. (2019) found optimal partitions across a wide range in terms of the number of modules, which suggests that there is no single number of clusters that most naturally represents the higher-order genetic structure of CT. Correlations in gene expression were higher within modules as opposed to between modules, and this was consistent across a range of modular resolutions (Alexander-Bloch et al., 2019). The authors interpret this multiscale modular structure as potentially indicative of a hierarchical organization where larger modules are at least partially composed of smaller modules across spatial scales.

Overall, genetic correlations are strongly influenced by the anatomical distance between brain regions such that the relationship is approximated by a quadratic polynomial (Figure 1A; Alexander-Bloch et al., 2019). Anatomical networks at whole-brain and cellular scales as well as functional networks in several species consistently demonstrate conservation of wiring costs and small-world topology (Vértes et al., 2012). Various explanations have been proposed for the ontogeny of this spatial constraint, including the increasing metabolic cost of connections between brain regions with increasing anatomical distance (Bullmore & Sporns, 2009). The total metabolic cost of building a physical connection and maintaining communication between brain regions increases with distance (Bullmore & Sporns, 2009). Lineage relationships of cortical neurons generated from proximal parts of the developing neuroepithelium may also explain the observed spatial constraint (Hawrylycz et al., 2012). It is possible that shared genetic variance results when neurons that comprise two regions derive from neural stem cells in similar germinal zones within the proliferative neuroepithelium at similar time periods (Hawrylycz et al., 2012).

For a physically embedded network like the brain, the distance penalization process that maintains the principle of spatial contiguity could be mediated mechanistically by the distance-related fall-off in concentration gradients of growth factors during fetal neurodevelopment (Alexander-Bloch et al., 2019). Animal studies support this molecular model of spatial constraints in genetic correlations. The mammalian cerebral cortex is divided into areas (arealization) early in neurogenesis by genes whose expression defines regional boundaries (Rubenstein & Rakic, 1999). The arealization of the cerebral cortex is initiated by patterning centers (e.g., anterior telencephalon) that secrete signaling molecules, which regulate the position and size of cortical areas (Rakic, 2009). This gradated expression of transcription factors in cortical progenitors is established by intrinsic genetic mechanisms. For example, fibroblast growth factor (FGF) has been shown to regulate the arealization of the cortex from a source in the anterior telencephalon (Rakic, 2009). Gene transfer in mouse embryos has been used to introduce a posterior source of FGF8, a member of the large FGF signaling family that is widely expressed during embryogenesis, and this perturbation profoundly changes the somatosensory map of the cerebral cortex (Fukuchi-Shimogori & Grove, 2001). This genetic manipulation leads to ectopic duplication of distinct cytoarchitectonic areas (i.e., somatosensory fields), supporting the role of signaling molecules in specifying positional identity during arealization. In addition, expression of the ID2 gene, a transcriptional regulator of cell differentiation in developmental pathways, respects the boundary of the sensory and motor cortex (Koppenhafer et al., 2022).

Regional specification in the cerebral cortex depends on interactions between intrinsic properties of cortical cells (i.e., gradients of signaling molecules established by gene expression) and input from subcortical structures such as the thalamus (Rubenstein & Rakic, 1999). According to the radial unit hypothesis, surface area is primarily driven by the number of radial

columns perpendicular to the surface of the brain, while cortical thickness is largely determined by the horizontal layers (including neurons and neuropil) during cortical development (Rakic, 2009). Genetically established gradients are responsible for directing axonal projections toward target neurons, forming a scaffolding along which neurons that populate the cortex migrate radially to their final locations in cortical layers II–VI (Winkler et al., 2010). Early area patterning is subsequently refined into disjunctive cortical maps based on neural activity as well as sensory and thalamocortical connections (O'Leary et al., 2007).Thalamocortical axon (TCA) input relays sensory information from the periphery to the cortex, and the differentiation of many anatomical features that distinguish cortical areas (e.g., architecture and distribution of output projection neurons) depend to a large extent on TCA input (O'Leary et al., 2007). Area-specific TCA targeting is likely primarily controlled intracortically by graded axon guidance molecules.

Additional organizational principles underlying the pattern of genetic correlations for cortical thickness appear to reflect maturation timing, primary versus association cortices, a priori functional boundaries, and neuroanatomical connectivity (Alexander-Bloch et al., 2019; Chen et al., 2013; Chen et al., 2008). Sensorimotor regions and the frontal, temporal, and occipital poles mature before higher-order association areas. Chen et al. (2013) found that the regions that matured early were grouped together in the same genetic clusters, despite some spatially discontinuity (e.g., primary motor merged with somatosensory clusters, anterior temporal merged with ventral frontal clusters including the frontal pole, and the two occipital clusters merged). The cross-regional genetic patterning of cortical thickness also partially corresponds to neuroanatomical connectivity. High genetic correlations between distal, noncontiguous regions may relate to underlying long-range fiber tract structures (e.g., thalamocortical or intracortical connections; Rimol et al., 2010). The modules identified by

Alexander-Bloch et al. (2019) and Chen et al. (2013) largely respect a priori functional boundaries. In particular, the medial occipital, dorsolateral prefrontal, ventromedial prefrontal, and limbic systems were all relatively well delineated (Figure 1B; Alexander-Bloch et al. 2019).

More recently, factor analyses have been used to formally model the genetic overlap across regional measures of cortical thickness within the Genomic Structural Equation Modeling (Genomic SEM) framework (Grotzinger et al., 2022). When conducting factor analyses, behavioral scientists often want to represent a large set of measured variables using a smaller, more parsimonious set of latent variables, while still preserving the essential information (e.g., correlations between variables) contained within the original data (Zwick & Velicer, 1982). Confirmatory factor analyses allow for the assessment of fit between observed data (i.e., a genetic covariance matrix) and an a priori theoretical model that specifies the hypothesized relations between latent factors and their observed indicator variables (i.e., individual brain regions; Loehlin & Beaujean, 2017). Genomic SEM is a recently developed statistical method that can model the shared genetic architecture of complex traits by applying traditional structural equation modeling principles to genetic covariances (Grotzinger et al., 2019). Characterizing the genetic correlations between brain regions serves as a step toward identifying novel phenotypes for genetic association studies of complex behavioral traits and providing etiological insights.

The Current Study

The current study capitalized on publicly available, summary-level data (i.e., summary statistics representing regression coefficients and their standard errors for the regression of each region's cortical thickness on each SNP) from a recent GWAS of cortical thickness conducted by the ENIGMA Consortium (Grasby et al., 2020). The aim of the current study was to model genetic correlations among regional measures of cortical thickness with latent dimensions. In

addition, tentative neurobiological hypotheses are advanced for this dimensional structure with suggestions for future efforts to characterize the resulting anatomical genetic dimensions.

Although the ENIGMA Consortium analyzed both surface area and cortical thickness in their genome-wide meta-analysis of neuroimaging phenotypes, CT was chosen as the primary structural index as the spatial distribution of heritability for surface area follows a more homogeneous pattern (Winkler et al., 2010). A larger degree of regional variation on genetic influences suggests that regional differences in thickness are more likely to reflect underlying, regional cytoarchitectonic differences (Winkler et al., 2010). In addition, unlike for surface area, controlling for total thickness had only a modest effect on regional heritabilities for thickness measures (Eyler et al., 2012). This is suggestive of unique genetic influences on regional CT that are not shared with the genetic factors that determine overall thickness of the cortex.

Genomic SEM was used to organize the 34 parcellated regions of cerebral cortex from the ENIGMA Consortium into anatomical genetic dimensions, or clusters of brain regions with shared genetic influences on cortical thickness via pleiotropy. Genomic SEM is a novel extension of linkage disequilibrium (LD) score regression that uses association statistics from genetic variants across the genome to estimate the genetic correlation between two traits of interest (Bulik-Sullivan et al., 2015). Genomic SEM fits structural equation models to genetic covariance matrices derived from GWAS summary statistics, without needing individual-level data. Genomic SEM also transforms different measures of effect sizes (e.g., beta, odds ratio) for harmonization across GWAS and importantly, accounts for the use of GWAS summary statistics from samples of varying and potentially unknown degrees of overlap (Grotzinger et al., 2019).

A heatmap of genetic correlations estimated using Genomic SEM across the cortical regions in the current study indicated pervasive overlap in associated genetic variants (Figure 2).

Based on this widespread pleiotropy and previous attempts to represent regional variation in CT, functional specificity and model fit was not wholly sacrificed for parsimony. A series of exploratory factor analyses (EFAs) were first estimated, where the regions freely loaded on 2, 3, 4, 5, 6, or 8 factors. All four variants of the 7-factor solution failed to run in Genomic SEM due to technical problems. A series of confirmatory factor analyses (CFAs) were then specified based on these EFAs and subsequently fit in Genomic SEM, for which model fits were compared in an effort to adjudicate between models and further examine those that appeared to best recapitulate the observed genetic correlations between regions. This analysis of the genome-wide architecture of cortical thickness is situated within and contributes to a larger effort to determine the biological, functional, and clinical relevance of varying levels of structural brain organization.

Methods

Summary Statistics: ENIGMA

The current study utilized publicly available summary statistics provided by the ENIGMA Consortium (Grasby et al., 2020) for regional cortical thickness averaged across both hemispheres in European ancestry individuals. Summary statistics are defined as the aggregate p-values and association data for every variant analyzed in a genome-wide association study (GWAS). Grasby et al. (2020) extracted measures of cortical thickness from in vivo whole-brain T1-weighted magnetic resonance imaging (MRI) scans using FreeSurfer MRI-processing software (Fischl, 2012). Global volume and mean CT were quantified for each individual across the whole cortex and cortical thickness was quantified within 34 distinct gyral-defined regions.

Regional boundaries were defined by the Desikan-Killiany atlas, which partitions the cortex based on gyral anatomy labeled from between the depths of the sulci (Desikan et al., 2006). Sulci are grooves or depressions in the cerebral cortex while gyri are ridges; together they

make up the characteristic folded appearance of the brain in humans and other mammals (Campero et al., 2014). Although the definitions of the regions of the Desikan-Killiany atlas follow macroanatomic landmarks, not cytoarchitectonic (i.e., at the cellular level) landmarks, there is evidence suggesting a substantial overlap between them. Whole-brain histology of postmortem human brains and surface-based analyses have demonstrated that cortical folding patterns align with changes in the laminar distribution of neuronal cell bodies (cytoarchitecture) and are able to predict the localization of Brodmann's areas (Fischl et al., 2008). The primary GWAS of regional measures included the global measure of mean thickness as a covariate to identify genetic variants specific to each region. The European ancestry sample included in the analyses conducted by Grasby et al. (2020) comprised 33,992 participants (23,909 from 49 cohorts in the ENIGMA Consortium and 10,083 from the UK Biobank; see Table 1).

Quality Control Procedures

Quality control filters for estimating the genetic covariance and sampling covariance matrices followed the defaults in the Genomic SEM (Grotzinger et al., 2019) implementation of linkage disequilibrium score regression (LDSC; Bulik-Sullivan et al., 2015). These filters included restricting to SNPs present in HapMap3 with information scores (INFO) > .9 and a minor allele frequency (MAF) > 1%. Approximately 90% of sequence variation among individuals is due to common variants (Gibbs et al., 2003). HapMap 3 is the third phase of the International HapMap project, which aims to characterize sequence variants, their frequencies, and correlations between them (Gibbs et al., 2003). MAF refers to the frequency at which the less common allele at a locus occurs in a given population. A SNP's MAF can have many effects on analyses as allele frequency is associated with the structure of local linkage disequilibrium (LD) and the relative size of the association statistic (i.e., regression coefficient for a SNP;

Coleman et al., 2016). LD refers to the nonrandom association of alleles at different loci, such that the alleles at neighboring polymorphisms on the same chromosome are associated within a population more often than if they were unlinked. SNPs were filtered by MAF as lower minor allele count limits the validity of conclusions drawn from analyses of SNPs.

GWAS use commercial SNP microarrays to genotype large numbers of genetic markers. However, SNP microarrays currently can only genotype up to one million of the 9–10 million common SNPs in the assembled human genome (Lin et al., 2010). Imputation infers untyped SNPs from known genotypes based on haplotypes from the International HapMap project, boosting power by increasing SNP coverage (Lin et al., 2010). Specific haplotypes reflect unique combinations of SNPs that reside near each other on a chromosome and tend to be inherited together. Poorly imputed data were filtered out based on INFO scores, which relate to the quality of the imputation for each variant. The linkage disequilibrium (LD) scores used for LDSC were calculated using the European subsample of the 1000 Genomes phase 3 project (Auton et al., 2015). SNPs in LD with a causal variant show elevated test statistics in association analysis proportional to the LD (measured by r^2) with the causal variant (Bulik-Sullivan et al., 2015). The LD score of a variant is defined as the sum of LD r^2 between that variant and all other variants in a 1 centimorgan (cM) region. LD scores excluded the major histocompatibility complex (MHC) region due to the high degree of LD outliers (i.e., loci with extensive long-range LD) in this region, as such outliers are known to have disproportionate and undue influence on estimates of genetic correlations produced from LD score regression (LDSC; Bulik-Sullivan et al., 2015).

Linkage Disequilibrium Score Regression

For two highly polygenic traits, the cross-trait genetic correlation can be calculated as the correlation of the genetic effects of numerous SNPs on the two traits (Bulik-Sullivan et al.,

2015). Genomic SEM is a novel extension of LD score regression, which can be used to produce SNP-based heritability estimates and calculate the genetic covariance among separate phenotypes using GWAS summary statistics (Grotzinger et al., 2019). SNP-based heritability measures the proportion of phenotypic variance explained by all measured SNPs in GWAS. The resulting variable in cross-trait LDSC is the product of two Z statistics (i.e., SNP effect size divided by its SE) for testing non-zero heritability, each taken from a GWAS of a distinct trait. Regression of these GWAS association statistics on LD scores partitions the statistics into a part that covaries with LD scores (the slope) and a part that does not (the intercept; Lee et al., 2018). The slope of LD score regression is proportional to the genetic covariance between the two traits of interest and the intercept is a useful measure of confounding (i.e., bias from sample overlap).

The bivariate LDSC intercept reflects the phenotypic correlation weighted by proportional sample overlap, thereby providing a quantitative index of the sampling dependence across the ENIGMA summary statistics (Bulik-Sullivan et al., 2015). Sample overlap (re-use of subjects between GWA studies) leads to non-independent data sets and in turn, spurious correlations between the summary statistics from two GWAS. Sample overlap only affects the intercept from bivariate LDSC and not the slope, so the resulting estimates of genetic correlation will not be biased by sample overlap. As such, any upward departure of the intercept from zero is indicative of confounding, which can then be corrected for so that estimates are not biased.

Using LD score regression, Genomic SEM estimates a genetic covariance matrix of all included traits, **S**, in which diagonal elements represent SNP-based heritability, and off diagonal elements represent genetic covariance between two variables (see Figure 2 for genetic heatmap). The estimation uncertainty is accounted for in a sampling covariance matrix, **V**, which contains squared standard errors of the estimates (genetic variances and covariances) in **S** on the diagonal

and the covariance between each pair of elements of **S** in the off diagonal. The off-diagonal elements of **V** capture potential sample overlap across traits (Grotzinger et al., 2019).

Exploratory Factor Analyses

In order to explore the full scope of factor solutions, exploratory factor analyses (EFAs) were used as a data-driven method of generating hypotheses to help guide the specification of alternative models for later structural equation modeling with Genomic SEM. Such a data-driven method was utilized as the patterns of genetic correlations between regional measures of cortical thickness have previously been shown to reflect multiple non-mutually exclusive organizing principles: spatial contiguity, bilateral symmetry, neuroanatomical connectivity, anatomic distance, functional boundaries, developmental/maturational timing, gradients of transcription factors (i.e., signaling molecules), and gene expression (Alexander-Bloch et al., 2019; Chen et al., 2013). EFAs were conducted using the *factanal* R package for two to eight factor solutions using the promax rotation (Beaujean, 2013). Promax is an oblique rotation that first assumes the factors are orthogonal and then relaxes the rotation to allow them to correlate (Russell, 2002). An oblique method was preferable to an orthogonal method due to theoretical reasons derived from prior research (i.e., SNPs associated with different brain regions are not entirely distinct).

Confirmatory Factor Analyses

Using Genomic SEM, confirmatory factor analyses (CFAs) specified on the basis of these EFAs were subsequently fit to the genetic covariance matrix (**S**) produced by LD score regression (Grotzinger et al., 2019). For the CFAs, individual regions were assigned to factors when the absolute value of their standardized loading (λ) exceeded 0.2 in the corresponding EFAs. Factor loadings can be interpreted like simple regression coefficients, representing the relationship of each variable to the underlying factor. If the absolute value of a brain region's

standardized loading did not achieve 0.2 for any factor, the region was assigned to the factor on which it had the standardized loading of the largest magnitude. For regions with evidence of cross-loadings ($|\lambda| > 0.2$ for 2 or more regions), these cross-loadings were included in the confirmatory models. Grotzinger et al. (2020) used 0.2 as a more lenient threshold for their previous investigation of the genome-wide factor structure of psychiatric traits. As such, it was selected as the standardized loading criterion for the current analyses so that the ability of confirmatory models to recapitulate the data (i.e., variance-covariance matrix) was not sacrificed in pursuit of parsimony. Additionally, a common factor model was tested to determine whether a single, general factor is sufficient to describe the data.

Models were estimated using unit variance identification (i.e., factor variances were fixed to 1) and the diagonally weighted least squares (DWLS) estimator as it incorporates the **V** matrix in model fitting (Grotzinger et al., 2019). For each of the two through eight factor solutions, four models were tested: an orthogonal factors model, correlated factors model, bifactor model, and modified bifactor model (Figure 3). The only difference between the orthogonal and correlated factor models specified based on the EFA results was that specific factors were not allowed to correlate in the former and were allowed to correlate in the latter. The bifactor models consisted of a general factor that captured shared genetic variation across the 34 brain regions, as well as orthogonal specific factors (defined by the same brain regions from the orthogonal and correlated factors models) that modeled residual genetic covariation not accounted for by the general factor. In the modified bifactor models, the specific factors were allowed to correlate with one another.

Confirmatory models were evaluated using a combination of goodness-of-fit statistics and model characteristics (average median factor loading, factor loading squared, and standard error of loadings). Goodness-of-fit statistics included the χ^2 statistic, Akaike information criteria

(AIC), comparative fit index (CFI), and standardized root mean square residual (SRMR). All four goodness-of-fit statistics are provided for each confirmatory model as per the defaults in Genomic SEM. χ^2 tests the null hypothesis that the variance-covariance matrix implied by a model is equal to the observed variance-covariance matrix. A non-significant result for this test typically indicates good model fit, thus it is desirable not to reject this null hypothesis. However, the χ^2 statistic is almost always statistically significant for models with larger sample sizes (e.g., >10,000 participants) as it becomes too sensitive to very small discrepancies between implied and obtained covariance matrices (Barrett, 2007). For the current analyses, χ^2 was used as a comparative measure of fit with lower values indicating better fit (Grotzinger et al., 2019). AIC was also used as a comparative fit index, with lower values again indicating better fit. AIC has similar problems to those of the χ^2 statistic since it is a simple transformation of χ^2 that adjusts for model complexity. As such, CFI and SRMR were additionally used to assess model fit.

CFI is an incremental fit index directly based on the non-centrality parameter, which is a measure of the degree to which a null hypothesis is false (Kirk, 2012). An incremental fit index such as CFI is analogous to R^2 and places the model being tested on a continuum between the fit of the worst possible model (null model, value of zero) and the fit of the best possible model (value of one). For CFA, the usual convention for the null or independence model is to allow all the variables in the model to have variation but no correlation and to have freely estimated means and variances. SRMR is defined as the standardized difference between the observed correlations and the model-implied correlations. It is presumed that the best fitting model has a SRMR of zero. CFI values greater than 0.9 and SRMR values less than 0.08 generally indicate good model fit (Hu & Bentler, 1999). However, Barrett (2007) and Hayduk et al. (2007) caution against strict reliance on cutoffs for acceptable fit and recommend detailed diagnostic investigations into

model characteristics. It should also be noted that a good-fitting model is not necessarily a valid model, thus parameter estimates were also carefully examined for each individual confirmatory model tested. For example, models with nonsensical results (e.g., standardized factor loadings or correlations greater than one, negative residual variances) can be "good-fitting" models.

Results

Linkage disequilibrium score regression applied to the ENIGMA summary statistics for the 34 bilateral averages of regional cortical thickness indicated pervasive genetic overlap across regions. Higher genetic correlations were observed among certain groups of cortical regions, for example, the occipital and cingulate cortices were relatively well delineated in the genetic heatmap (Figure 2). This LDSC correlation structure was formally modeled by first estimating exploratory factor analyses with two through eight-factor solutions, as described above. A series of confirmatory factor models were subsequently fit using Genomic SEM and specified based on these EFAs, also as described above (see Table 2 for fit statistics of all models tested).

Based on fit statistics alone, the modified bifactor model consisting of a general factor and eight correlated specific factors that modeled covariation not accounted for by the general factor was the best "fitting" model (χ^2[418] = 491427762, AIC = 491427762, CFI = 0.781, SRMR = 0.073). However, close examination of the full model output revealed that multiple standardized factor loadings were estimated as larger than one, rendering this factor solution invalid, or at least implausible. The next best model based on fit statistics alone was the bifactor model with eight orthogonal specific factors (χ^2[466] = 605755437, AIC = 605755437, CFI = 0.730, SRMR = 0.088; see Table 4 for factor loadings). It is important to note that on average, a given bifactor confirmatory model will tend to fit better than other models (e.g., a correlated factor model) regardless of the true data generating process in the population (Markon, 2019).

The tendency of bifactor models to flexibly fit (or overfit) any dataset better, independent of the population model, is partly accounted for by their greater number of parameters (Markon, 2019). Bifactor models are more likely to capture chance features of any given dataset that might not replicate (Markon, 2019). As such, bifactor models are prone to positive bias in model selection.

Fit statistics and a lack of nonsensical parameter estimates can only provide so much information regarding local model fit. As such, Waldman and colleagues have advocated for the use of alternative additional indices to augment standard model fit statistics (Waldman et al., 2022). For the 24 confirmatory models that successfully ran and converged in Genomic SEM, these additional indices were calculated: the mean, median, and standard deviation of the standardized factor loadings (λs), standard error (SE) of λs, and squared λs for each factor, which reflect the percentage of variance in a variable explained by the factor. In addition, the median of these three statistics calculated per factor were (1) averaged across all factors in the orthogonal and correlated factors models or (2) averaged across only specific factors and also across all factors including the general factor in the bifactor and modified bifactor models. The eight correlated factors model had a larger average median factor loading and factor loading squared, but also a higher average median standard error of loadings across all factors ($\overline{Med}$ λ = 0.435, $\overline{Med}$ SE of λ = 0.126, $\overline{Med}$ λ^2 = 0.199) compared to the bifactor model with eight specific factors averaged across specific factors ($\overline{Med}$ λ = 0.330, $\overline{Med}$ SE of λ = 0.104, $\overline{Med}$ λ^2 = 0.116) and across all factors ($\overline{Med}$ λ = 0.329, $\overline{Med}$ SE of λ = 0.103, $\overline{Med}$ λ^2 = 0.115; Table 3). The eight factors in the correlated factors model had low genetic correlations between them (average absolute value of factor intercorrelation r_g = 0.251), which could be evidence of relatively distinct genetic underpinnings for each of the eight factors. On the other hand, it is also potential evidence of an overfactored solution, or a solution with too many cross-loadings (individual

brain regions loading on two or more factors). Both the eight correlated factors and bifactor models represent viable contenders for the best fitting model based on examination of goodness-of-fit statistics, parameter estimated, and model characteristics and were considered further.

Discussion

The current study examined the multivariate genomic architecture of cortical thickness and identified eight specific latent factors using the largest available neuroimaging genomic dataset (Thompson et al., 2019). Exploratory and confirmatory factor analyses of the genetic covariance between measures of regional cortical thickness revealed a higher-order structure that respected many of the organizing principles demonstrated in the literature. Consistent with prior findings (Alexander-Bloch et al., 2019; Chen et al., 2013), novel genomic factors of the cortex were largely topologically clustered. Most exceptions to the principle of spatial contiguity for regions within a factor have been previously shown to have either indirect or direct connectivity, whether functional or structural (Makris et al., 2005). The regional composition of the eight specific factors in the correlated factors and bifactor models (Figure 4) also reflected high genetic correlations among primary cortices (i.e., visual, motor, somatosensory cortices) compared to between primary and association cortices. The findings of the current study were examined in the broader context of the neuroimaging literature to better understand these novel factor structures. Characterizing the biological, functional, and clinical relevance of these novel brain factors is a necessary step before using these factors to gain mechanistic insight into complex traits. Ultimately, these latent brain factors can be used as novel phenotypes to reveal the extent to which genetic variants that influence the development of specific cortical regions also influence outcomes like the development of personality and risk for psychopathology.

Characterization of Resulting Genomic Factors

When considering the general factor in the bifactor models tested, it is important to note that the GWAS summary statistics from the ENIGMA Consortium used in the current study included a global measure of mean thickness as a covariate. Although global brain structure is highly heritable, considerable regional variability in the magnitude of genetic influences on cortical thickness has been demonstrated in previous analyses (Winkler et al., 2010). Rimol et al. (2010) investigated the heritability of cortical thickness on a continuous basis across the entire cortical surface and found strong evidence of regionally-specific patterns rather than a single, global genetic factor. Additionally, Rimol et al. (2010) demonstrated that regional patterns of genetic correlations were largely consistent with a division between primary and association cortex, as well as broadly-defined patterns of brain gene expression, neuroanatomical connectivity, and brain maturation trajectories. The analytic pipeline of the current study adjusted for global covariance in order to utilize region-specific genetic variants, with the aim of identifying maximally separable genetic dimensions with distinct sets of brain regions. This analytic pipeline has the disadvantage of introducing potential bias by adjusting for a heritable trait (i.e., average CT), complicating the interpretation of a general factor in the bifactor models.

The difficulty of estimating direct effects of genetic variants on a covariate-adjusted outcome is well appreciated in causal inference literature (Aschard et al., 2015). When adjusting for a covariate that has a genetic component, the adjusted association signals do not necessarily imply an association with regional thickness only but can correspond also to a bivariate signal on mean thickness and regional thickness (Aschard et al., 2015). The average bias of the genetic effect estimate in a covariate-adjusted analysis is a function of the correlation between the outcome and the covariate. If the effect of a genetic variant on thickness in a particular region

and the phenotypic correlation between CT in that region and mean thickness globally are in the same direction, the adjusted statistical test may have decreased power to detect the genetic variant as compared to the unadjusted test (Aschard et al., 2015). Conversely, if the genetic effect and the phenotypic correlation are in opposite directions, the adjusted statistical test can have increased power to detect the genetic variant when there truly is a direct genetic effect on the outcome (Aschard et al., 2015). In theory, global covariation is accounted for by modeling a latent general factor in the bifactor models (Loehlin & Beaujean, 2017). This interpretation is cautioned against in this case as the analytic pipeline adjusted for global covariation in CT.

The observed patterns of genetic correlations and the resulting factor structure with respect to the eight specific factors does not lend itself to any simple interpretation in terms of cortex type or functional systems, as it appears to reflect many processes in combination. The results of the current study are consistent with multiple genetic factors with different, but partially overlapping patterns of influence, and like prior investigations of the genetic architecture of cortical thickness, no single explanation appears to be sufficient. Overall, the patterns of genetic correlations between regional measures of cortical thickness did not conform to traditionally-defined brain structure boundaries (e.g., lobular divisions, preservation of individual brain regions from the sulcal-based Desikan-Killiany atlas; Desikan et al., 2006). As such, the following review of neuroscience literature is intended to highlight possible interpretations for the distribution of brain regions across the eight factors (Figure 4).

The eight specific genomic brain factors found in the current study appear to reflect several non-mutually exclusive organizing principles such as anatomical distance and structural and functional connectivity, similar to the findings of previous investigations (Alexander-Bloch et al., 2019; Chen et al., 2013). For example, the superior parietal cortex is heavily

interconnected (both anatomically and functionally) with the caudal middle frontal gyrus (Koenigs et al., 2009), and both regions loaded on Factor 2. Many neurons in the orbitofrontal cortex receive major visual input and are thought to represent the reinforcement association of visual stimuli (Rolls, 2004). In the current study, the medial orbitofrontal cortex and the occipital lobe both loaded on Factor 5. Regions in the prefrontal cortex (i.e., pars triangularis and opercularis, rostral middle frontal gyrus, superior frontal gyrus) loaded negatively on Factor 3 while regions in the inferior parietal cortex had positive loadings on Factor 3. The negative factor loadings for prefrontal regions suggests that genetic variants that contribute to the expansion of CT in the inferior parietal cortex tend to also contribute to thinner cortex in prefrontal regions. The high genetic correlations between prefrontal cortex and inferior parietal cortex thickness might be accounted for by anatomical connectivity as they are at essentially at opposite ends of the dorsal component of the superior longitudinal fasciculus, a major intrahemispheric fiber tract (Makris et al., 2005). The occipitofrontal fasciculus extends rostrally to the superior frontal gyrus and premotor cortices (e.g., caudal middle frontal gyrus) and caudally to the precuneal area and the inferior parietal lobule (Makris et al., 2007). The superior and caudal middle frontal gyri as well as the precuneus and inferior parietal cortex all loaded on Factor 2. Makris et al. (2007) suggested a putative role for the occipitofrontal fasciculus in focusing attention in visual space by virtue of its connections with areas shown to play a role in visuospatial function. The role of structural connectivity in explaining genetic correlations among regional CT measures is unsurprising, as CT has been well-established as reflecting the elaboration of cortical circuitry.

Overall, the eight specific factors found in the current study appear to reflect a biologically relevant partitioning of the cortex. Of the putative organizing principles suggested to underlie the patterns of interregional genetic correlations, structural connectivity appears to be

more well-justified by the neuroimaging literature compared to functional specificity. It can be problematic to infer the involvement of a specific cognitive process from the activation of a brain region (or co-activation of regions), and this kind of reasoning is known as "reverse inference." Reverse inference has been previously criticized on the basis that it does not take into account how selectively the area is activated by the mental process in question (Hutzler, 2014). As specific brain region can be activated by a wide range of cognitive processes, functional interpretations of the specific factors found in the current study are cautioned against until additional functional neuroimaging resources (i.e., databases, metadata) are well developed.

A more recent approach known as multivoxel pattern analysis (MVPA) can be used to formally test the ability to infer mental states from neuroimaging data. This approach uses tools from the field of machine learning to create statistical machines that can accurately decode the mental state that is represented by a particular imaging data set (large-scale decoding; Poldrack, 2011). Major challenges for large-scale decoding are the lack of a sufficient database of raw functional MRI data and the scarcity of detailed metadata describing the tasks and processes associated with each data set (Poldrack, 2011). The development of large databases of task-based fMRI data such as the OpenfMRI project will help provide the data needed for such decoding analyses (Poldrack & Gorgolewski, 2017). Poldrack and colleagues are also currently developing a knowledge base that will serve as a framework for detailed annotation of neuroimaging databases as part of the Cognitive Atlas Project (Poldrack et al., 2011). Until these resources are well developed, the ability to classify mental states on a larger scale is largely theoretical.

Cortical Thickness, Psychopathology, and Personality

Genes presumably play a role in personality and psychopathology via involvement in the development and function of brain regions responsible for specific cognitive and emotional

processes (Rasetti & Weinberger, 2011). Endophenotypes are heritable, co-segregate with the disorder within families of patients, and reflect the actions of genes predisposing an individual to a disorder, even in the absence of diagnosable pathology (Miller & Rockstroh, 2013). Alterations in brain structure are promising candidate endophenotypes for psychopathology, as gray matter characteristics have been shown to be highly heritable (Winkler et al., 2010) and a multitude of studies have demonstrated abnormalities of brain structure in psychiatric disorders.

Phenotypic correlations with regional measures of cortical thickness have been reported for ADHD (Almeida Montes et al., 2013), anxiety disorders (Bas-Hoogendam et al., 2018; Frick et al., 2013; Gold et al., 2017; Molent et al., 2018), obsessive-compulsive disorder (Fouche et al., 2017), anorexia nervosa (Fuglset et al., 2016; Lavagnino et al., 2018), bipolar disorder (Hanford et al., 2016), conduct disorder (Hyatt et al., 2012), post-traumatic stress disorder (Wrocklage et al., 2017), antisocial personality disorder (Jiang et al., 2016), autism spectrum disorder (Khundrakpam et al., 2017), major depressive disorder (Li et al., 2020), and schizophrenia (Yan et al., 2019). However, statistical association of neuroimaging phenotypes with psychiatric diagnosis alone does not establish a mechanism of risk from brain-relevant genetic polymorphisms to the development of psychopathology (Bigos & Weinberger, 2010).

Recent analyses suggest that genes that confer relatively broad liability to multiple psychiatric disorders act on neurodevelopment and the establishment of brain circuitry and additionally show heightened expression in the brain throughout the lifespan (i.e., not only in early brain development; Lee et al., 2019). Genome-wide significant loci associated with risk for multiple psychiatric disorders as well as genome-wide significant loci associated with regional measures of cortical thickness both play prominent roles in neurodevelopmental pathways (Grasby et al., 2020; Lee et al., 2019). Broad, generalized genetic risk for psychopathology may

shape the phenotypic (i.e., cognitive, affective) expression of psychiatric disorders by affecting brain structure and function, and ultimately behavior. Isolating the neural substrates of such genetic vulnerability is a necessary step toward characterizing the pathophysiological mechanisms that are shared across psychiatric disorders or unique to individual disorders.

In the domain of personality, quantitative genetic analyses have recently demonstrated that shared genetic influences underlie the association between five-factor model (FFM) traits and local cortical structure (Valk et al., 2020). Personality traits are associated with a wide range of outcomes including physical health and subjective well-being, psychopathology, interpersonal relationships, occupational outcomes, and criminal activity (Ozer & Benet-Martínez, 2006). Genetic correlations have been found between Agreeableness and bilateral superior frontal gyrus CT, Openness and right temporal pole CT, and Neuroticism and right superior and lateral frontal CT (Valk et al., 2020). Genetic correlations between FFM traits and prefrontal regions may reflect the link between personality and high-level socio-cognitive and affective processes. Genetic variants that influence regional CT have recently been associated with complex cognitive abilities (Grasby et al., 2020). Further, cortical thickness of the left rostral middle frontal gyrus has been found to significantly mediate the relation between genetic variants and Neuroticism (Song et al., 2021). Overall, personality-related genetic variants are mainly involved in brain development, have the highest expression in the frontal cortex, and influence CT in key regions for emotion processing and regulation (Adelstein et al., 2011; Allen & Deyoung, 2016; Song et al., 2021; Valk et al., 2020; Yarkoni, 2015). Efforts to describe the emergence of personality have consistently implicated neural characteristics, but the extent to which regional cortical structure and personality share a genetic basis remains unclear. The specific factors

resulting from the current analyses can aid in phenotype definition for genetic association studies that examine the shared genetic basis of brain structure and personality and psychiatric traits.

Limitations

The current analyses have a number of limitations that should be noted. Primarily, additional analytic work is necessary to test alternative factor structures before resulting specific factors are used in future studies examining the relation between such cortical phenotypes and behavioral traits. Follow-up analyses that build on the current study will test alternative factor structures to try and determine the one in which the factors are the most reliable and valid. It is of note that the cortical thickness data from the ENIGMA Consortium reflects an heterogeneous sample ranging in age from 12 to 90 years old, and findings should be interpreted with this in mind (Grasby et al., 2020). CT is thought to reflect phenomena taking place in cortical maturation during intrauterine development (i.e., asymmetric division of progenitor cells; Rakic, 2009) and during childhood and adolescence such as dendritic arborization, synaptic and axonal pruning, myelination, and apoptosis (Shaw et al., 2008; Vanderhaeghen & Cheng, 2010). There is also cross-sectional evidence that the extent of genetic and environmental influences on brain structure may change throughout childhood and adolescence (Rimol et al., 2010). Further study of patterns of genetic correlations among brain structural metrics is warranted to determine whether and how such patterns change across development. Another limitation of the ENIGMA Consortium data is that measures of CT were averaged across both hemispheres for each individual participant (Grasby et al., 2020). Hemispheric anatomical asymmetries and the lateralization of brain function (i.e., the tendency for some neural functions or cognitive processes to be specialized to one side of the brain or the other) have been shown to appear very early in life (Tzourio-Mazoyer et al., 2020). It is critical that factor analytic models of CT

continue to be evaluated in genetically informed neuroimaging datasets with more specific developmental windows and with separate summary-level data for each cerebral hemisphere.

It must be highlighted that the results of the current study results are restricted to participants of European ancestry due to the availability of sufficiently well-powered GWAS data for this ancestral group. Many genome-wide association studies have been limited to subjects of a single ancestry to prevent population stratification due to race and ethnicity, or differences in LD structure across different populations. As such, it is a requirement of LD-score regression to produce estimates within a single ancestral population (Bulik-Sullivan et al., 2015). A goal of the current program of research is to include emerging samples that better reflect the world's genetic diversity, with future analyses building on genetically informed datasets in non-European ancestry populations. Without such representation in future analyses, the application of discoveries from neuroimaging genetics to improve research and society will be limited.

Lastly, the analytic pipeline used in the current study may have introduced bias due to adjusting for a global metric of CT (i.e., mean thickness), which is a heritable trait. For example, it was not possible in the current study to equivocally determine whether a genetic correlation between mean thickness and regional thickness results from a direct effect of mean thickness on regional thickness (Aschard et al., 2015). Grotzinger et al. (2022) also modeled the multivariate genomic architecture of CT by applying Genomic SEM to summary statistics of regional CT from the ENIGMA Consortium. In contrast to the current study, Grotzinger et al. (2022) used summary statistics (Grasby et al., 2020) that were not corrected for a global structural metric and also assigned individual brain regions to a factor based on a more stringent threshold (EFA standardized factor loadings greater than .5). Grotzinger et al. (2022) found that a five-factor correlated factors model and bifactor model with five orthogonal specific factors both fit the data

well. By using unadjusted summary statistics, Grotzinger and colleagues were able to explicitly model the shared genetic variation across the 34 regions in the context of a bifactor model (Grotzinger et al., 2022). By using a more stringent threshold, their confirmatory factor models did not include any cross-loadings and in turn, the five factors in their correlated factors model were highly genetically correlated (average factor r_g = .80; Grotzinger et al., 2022).

Future Directions

A future goal of the present program of research is to conduct the analyses of the current study again but with unadjusted summary statistics instead, so that global covariation can be explicitly accounted for by modeling a latent general factor in the bifactor models. At the same time, using the unadjusted summary statistics for regional cortical thickness would allow for a more psychometrically informed comparison with the findings of Grotzinger et al. (2022). Grotzinger and colleagues aimed to determine the number of genomic factors that could most parsimoniously represent the ENIGMA Consortium data (Grasby et al., 2020) and primarily sought to identify maximally separable genetic dimensions. As such, the authors applied several tests to the genetic correlation matrices derived from Genomic SEM, which pointed to a five-factor solution (Grotzinger et al., 2022). Based on these tests, the authors conducted exploratory and confirmatory factor analyses only for: (1) a general factor solution, and (2) for the five-factor solutions. The current study aimed to not only parsimoniously model the genetic architecture of regional cortical thickness, but also to define cortical phenotypes that would facilitate future genomic investigation into complex behavioral traits. As such, the fit and construct validity of two through eight factor solutions was examined. Ultimately, further factor analyses of the ENIGMA cortical thickness data without global adjustments will need to examine a continuum of factor loading thresholds rather than using only one threshold for model specification.

To resolve any differences between the findings of Grotzinger et al. (2022) and those of the current study, future analyses will use the set of ENIGMA summary statistics that were not corrected for mean thickness (Grasby et al., 2020) and assign individual brain regions to a factor based on thresholds for EFA standardized factor loadings ranging from |0.2| to |0.5|. The current study used additional indices of model fit such as the mean, median, and standard deviation of the standardized factor loadings (λs), standard error (SE) of λs, and squared λs for each factor. As these indices were not calculated by Grotzinger et al. (2022), they will be estimated for their five-factor solution using factor loadings that were provided. The validity of factor solutions resulting from future reanalysis of the ENIGMA data can be compared to the validity of Grotzinger and colleagues' solution by examining the patterns of genetic correlations with external variables for each set of factors. Grotzinger et al. (2022) observed no significant genetic relationships between their regional CT factors and psychiatric traits after correcting for multiple comparisons. This is in contrast to prior findings from quantitative genetic analyses that have demonstrated genetic correlations between regional measures of cortical thickness and various personality traits (Valk et al., 2020) as well as psychiatric phenotypes (Grasby et al., 2020).

Ultimately, the strength of imaging genetics and genomics lies in its translational and integrative potential with other research approaches (e.g., non-human animal models, psychiatric genetics) to elucidate brain-based pathways that give rise to the vast individual differences in behavior as well as risk for psychopathology. Grotzinger and colleagues' parsimony driven best fitting model is of limited utility for future genomic investigation into psychological traits due to its lack of genetic associations with external variables of interest. Imaging genetics and genomics can inform the neural mechanisms through which genetic and molecular differences impact cognition, emotion, and behavior in health and disease (Bogdan et al., 2017). However, valid

neurobiological phenotypes are a prerequisite for the appropriate application of the neurogenetic approach, which future analyses built on the current study will aim to generate and define.

The cerebral cortex is a complex structure with many functional cortical areas that are distinguishable by differences in gene expression (Hawrylycz et al., 2012), morphology (Valk et al., 2020), and connectivity (O'Leary et al., 2007). Collectively, the results of the current study indicate that the pervasive genetic overlap across regional measures of CT is not reflective of a single dimension of macroscale organization. It will be important for future studies to examine the multivariate genomic factor structure of cortical thickness found in data from the ENIGMA Consortium as well as in independent samples to demonstrate its portability and replicability. Future studies should also more quantitatively characterize brain factors before examining the genetic associations between such factors and facets of personality and psychiatric disorders.

Another critical future direction in the current program of research is to better understand the spatial organization of genomic brain factors by characterize their relationships with established molecular, cellular, and functional topographical maps. Similar to the methodology of Grotzinger and colleagues, the statistical significance of observed spatial correspondence between the boundaries defined by the present brain factors and those of canonical and meta-analytic maps from the neuroimaging literature can be assessed (Grotzinger et al., 2022). Maps used in future analyses could include cortical maps derived from the BigBrain project (intracortical microstructure, laminar differentiation, cellular and neuronal density derived from post-mortem brain histology; Amunts et al., 2013), cell-type specific transcriptional signatures from the Allen Human Brain Atlas (Hawrylycz et al., 2012), cortical association maps obtained from Neurosynth (a platform for the automated meta-analyses of fMRI studies; Yarkoni, 2015), network maps of anatomical connectivity from the Human Connectome Project (Van Essen &

Glasser, 2016), cytoarchitectural classes (e.g., granular, agranular cortex) defined by von Economo and Koskinas (Triarhou, 2007; von Economo & Koskinas, 1926), and functional intrinsic connectivity networks derived from resting-state functional magnetic resonance imaging (Yeo et al., 2011). Such future studies could capitalize on the recently developed ENIGMA Toolbox, an open platform for contextualizing neuroimaging data such as surface maps with respect to both microscale and macroscale brain organization (Larivière et al., 2021).

Conclusion: In Search of Mechanistic Understanding

The overarching long-term goal of this research program is to integrate genomics with neuroscience to better understand complex behavioral traits such as personality and psychopathology. An important aspect of the current study is that the resulting factor solutions based on interregional genetic correlations do not map directly onto traditional parcellation schemes. The results suggest that different sets of genes influence different subregions, as such, regions bounded by traditional parcellation units may be of limited utility for genome-wide association studies. While the current analyses do not represent an exhaustive assessment of the patterns of genetic influences on cortical thickness, this approach appears to be promising.

Characterizing patterns of genetic correlations among regional measures of brain structure has important implications for phenotype or neurobiological endophenotype definition in genetic association studies of complex behavioral traits. Factor analysis of patterns of genetic correlations can generate novel parcellation schemes with novel phenotypes. These novel phenotypes may be better suited than more traditional brain structure phenotypes for use in neuroimaging genetic studies of psychiatric and neurological disorders. In addition, characterizing such factors can aid in the development of rodent and possibly non-human primate models of cortical dysgenesis (i.e., aberrant cortical development) that mimic specific

genetic cortical disorders in humans. While scientific understanding of the genetic underpinnings of complex human traits remains limited, the current findings contribute to elucidation of the genetic architecture of the cerebral cortex, which has great potential to facilitate future genomic investigation into diverse traits. Joint analysis of summary-level data from different GWAS (i.e., GWAS of brain structure and GWAS of psychiatric disorders) provides new opportunities for further analyses and novel genetic discoveries, such as the shared genetic basis of complex traits.

Table 1

Sample Size for Each Region Included in Grasby et al. (2020)

Lobe	Cortical Region	Sample Size (Maximum)
Frontal	Frontal Pole	33,217
Frontal	Medial Orbitofrontal	32,165
Frontal	Lateral Orbitofrontal	32,541
Frontal	Rostral Anterior Cingulate	33,150
Frontal	Caudal Anterior Cingulate	33,193
Frontal	Superior Frontal	32,672
Frontal	Rostral Middle Frontal	32,727
Frontal	Pars Orbitalis	33,145
Frontal	Pars Triangularis	33,094
Frontal	Pars Opercularis	33,078
Frontal	Caudal Middle Frontal	33,093
Frontal	Paracentral	33,071
Frontal	Precentral	32,185
Parietal	Postcentral	31,681
Parietal	Precuneus	33,151
Parietal	Superior Parietal	32,481
Parietal	Supramarginal	31,908
Parietal	Inferior Parietal	32,850
Parietal	Posterior Cingulate	32,954
Parietal	Isthmus Cingulate	32,914
Temporal	Insula	32,396
Temporal	Entorhinal	31,894
Temporal	Parahippocampal	32,184
Temporal	Fusiform	32,927
Temporal	Temporal Pole	32,275
Temporal	Inferior Temporal	32,740
Temporal	Middle Temporal	31,707
Temporal	Superior Temporal	30,739
Temporal	Banks of the Superior Temporal Sulcus	30,879
Temporal	Transverse Temporal	33,095
Occipital	Lingual	32,381
Occipital	Pericalcarine	31,688
Occipital	Cuneus	32,187
Occipital	Lateral Occipital	32,782

Note. As certain SNPs were not present across all cohorts that comprise the ENIGMA consortium, the SNP-specific participant sample sizes were used for LDSC estimation. Sample size for each region ranged from 10,000 participants per associated SNP to indicated maximum.

Table 2

Model Fit for Confirmatory Factor Models from Genomic SEM

MODEL	χ^2	χ^2 df	χ^2 $p-val$	AIC	CFI	SRMR
General Factor	1392355275	527	0	1392355411	0.3801995	0.1378533
2 Orthogonal Factors	1549573381	519	0	1549573533	0.3102146	0.1408347
2 Orthogonal Bifactor	1142782568	485	0	1142782788	0.4912957	0.115343
2 Correlated Factors	1295496316	518	0	1295496470	0.4233158	0.1276197
2 Correlated Bifactor	1065267467	484	0	1065267689	0.5258012	0.1118263
3 Orthogonal Factors	1416492606	511	0	1416492774	0.3694549	0.1359495
3 Orthogonal Bifactor	991328416	477	0	991328652	0.5587148	0.1090587
3 Correlated Factors	1087410676	508	0	1087410850	0.5159442	0.1152334
3 Correlated Bifactor	904008750	474	0	904008992	0.5975848	0.1007764
4 Orthogonal Factors	1308575969	504	0	1308576151	0.4174935	0.129094
4 Orthogonal Bifactor	862016669	470	0	862016919	0.6162773	0.09812971
4 Correlated Factors	1063765017	498	0	1063765211	0.52647	0.1086745
4 Correlated Bifactor	790925514	464	0	790925776	0.6479233	0.09273192
5 Orthogonal Factors	1267043402	496	0	1267043600	0.4359815	0.1294562
5 Orthogonal Bifactor	850949443	462	0	850949709	0.6212039	0.09655158
5 Correlated Factors	952510340	486	0	952510558	0.5759945	0.1010421
5 Correlated Bifactor	753971614	452	0	753971900	0.6643731	0.08661038
6 Orthogonal Factors	1100964252	491	0	1100964460	0.5099109	0.1207096
6 Orthogonal Bifactor	658537208	457	0	658537484	0.7068553	0.08978156
6 Correlated Factors	849633697	476	0	849633935	0.6217896	0.09491048
8 Orthogonal Factors	1128543085	480	0	1128543315	0.4976343	0.1203329
8 Orthogonal Bifactor	605755437	446	0	605755735	0.7303509	0.08795653
8 Correlated Factors	681329255	452	0	681329541	0.6967095	0.08275341
8 Correlated Bifactor	491427762	418	0	491428116	0.7812433	0.07283355

Note. Orthogonal bifactor model refers to a simple bifactor model, correlated bifactor to a modified bifactor model. The standardized 6 factor modified bifactor model failed to converge, indicating more general problems with the model solution such as misspecification. All four variants of the 7-factor solution failed to run in Genomic SEM due to technical errors. χ^2 *p*-val and χ^2 df refer to the *p*-value and degrees of freedom for the model χ^2. AIC = Akaike information criteria; CFI = comparative fit index; SRMR = standardized root mean square residual.

Table 3

Alternative Fit Indices for Eight Factor Confirmatory Models

	Standardized Factor Loadings (λ)			SE of Factor Loadings			Factor Loadings Squared (λ^2)		
MODEL	**Mean**	**Median**	**SD**	**Mean**	**Median**	**SD**	**Mean**	**Median**	**SD**
8 Orthogonal Factors									
Factor 1	0.530	0.613	0.178	0.079	0.076	0.012	0.310	0.376	0.180
Factor 2	0.372	0.376	0.161	0.102	0.097	0.019	0.162	0.141	0.120
Factor 3	0.332	0.346	0.220	0.106	0.099	0.015	0.150	0.120	0.144
Factor 4	0.361	0.356	0.215	0.093	0.094	0.010	0.173	0.127	0.160
Factor 5	0.423	0.424	0.206	0.090	0.090	0.004	0.216	0.180	0.183
Factor 6	0.417	0.464	0.267	0.084	0.084	0.012	0.237	0.215	0.219
Factor 7	0.335	0.380	0.196	0.129	0.138	0.018	0.145	0.145	0.126
Factor 8	0.495	0.398	0.320	0.131	0.122	0.038	0.322	0.162	0.398
Average (ALL Factors)	0.408	0.420	0.220	0.102	0.100	0.016	0.214	0.183	0.191
8 Orthogonal Bifactor									
General Factor	0.303	0.321	0.190	0.093	0.091	0.015	0.127	0.103	0.140
Factor 1	0.404	0.447	0.210	0.097	0.094	0.011	0.204	0.200	0.175
Factor 2	0.339	0.335	0.143	0.102	0.099	0.017	0.134	0.112	0.120
Factor 3	0.306	0.333	0.225	0.103	0.098	0.016	0.135	0.111	0.138
Factor 4	0.277	0.209	0.230	0.111	0.107	0.018	0.125	0.044	0.227
Factor 5	0.416	0.403	0.207	0.092	0.092	0.007	0.211	0.163	0.176
Factor 6	0.298	0.224	0.297	0.089	0.087	0.012	0.167	0.050	0.274
Factor 7	0.322	0.292	0.186	0.124	0.126	0.021	0.134	0.085	0.131
Factor 8	0.464	0.398	0.265	0.134	0.132	0.032	0.268	0.166	0.290
Average (ALL Factors)	0.348	0.329	0.217	0.105	0.103	0.017	0.167	0.115	0.186
Average (SPECIFIC)	0.353	0.330	0.220	0.106	0.104	0.017	0.172	0.116	0.192
8 Correlated Factors									
Factor 1	0.507	0.584	0.202	0.103	0.087	0.038	0.295	0.341	0.172
Factor 2	0.521	0.500	0.313	0.194	0.202	0.094	0.362	0.250	0.374
Factor 3	0.399	0.341	0.269	0.150	0.141	0.036	0.244	0.118	0.306
Factor 4	0.399	0.404	0.251	0.150	0.132	0.076	0.217	0.164	0.280
Factor 5	0.427	0.341	0.190	0.100	0.091	0.024	0.215	0.117	0.181
Factor 6	0.414	0.356	0.230	0.097	0.096	0.011	0.219	0.127	0.231
Factor 7	0.365	0.390	0.280	0.158	0.137	0.088	0.200	0.152	0.245
Factor 8	0.510	0.561	0.246	0.120	0.118	0.014	0.305	0.322	0.225
Average (ALL Factors)	0.443	0.435	0.248	0.134	0.126	0.047	0.257	0.199	0.252
8 Correlated Bifactor									
General Factor	0.282	0.262	0.176	0.101	0.099	0.018	0.110	0.069	0.119
Factor 1	0.439	0.456	0.245	0.104	0.104	0.015	0.248	0.208	0.240
Factor 2	0.732	0.538	0.512	0.294	0.287	0.182	0.777	0.289	1.031
Factor 3	0.564	0.514	0.327	0.274	0.288	0.151	0.513	0.264	0.716
Factor 4	0.393	0.267	0.434	0.314	0.301	0.193	0.327	0.072	0.782
Factor 5	0.471	0.467	0.142	0.104	0.096	0.016	0.240	0.218	0.139
Factor 6	0.374	0.286	0.239	0.093	0.089	0.012	0.191	0.082	0.209
Factor 7	0.400	0.389	0.251	0.197	0.175	0.067	0.214	0.151	0.205
Factor 8	0.512	0.598	0.236	0.134	0.134	0.030	0.304	0.358	0.195
Average (ALL Factors)	0.463	0.420	0.285	0.179	0.175	0.076	0.325	0.190	0.404
Average (SPECIFIC)	0.486	0.439	0.298	0.189	0.184	0.083	0.352	0.205	0.440

Note. Mean, median, standard deviation (SD) of standardized factor loadings (λs), standard error of λs, and squared λs are shown, as well as averages across all factors and only specific factors.

Table 4

Confirmatory Factor Results from Cortical Thickness Measurement Model

			Region of Cerebral Cortex	GEN	FAC 1	FAC 2	FAC 3	FAC 4	FAC 5	FAC 6	FAC 7	FAC 8
TEMPORAL LOBE		MEDIAL ASPECT	Entorhinal Cortex	-0.24**				-0.38***				
			Parahippocampal Cortex	-0.33***			0.34***	-0.23*			-0.29**	
			Temporal Pole	-0.33**		-0.46***				-0.22*	-0.33**	
			Fusiform Gyrus	-0.35***		-0.23	0.02				-0.29*	
		LATERAL ASPECT	Superior Temporal Gyrus	0.16		-0.69***						
			Middle Temporal Gyrus	-0.13		-0.19	0.15					0.49**
			Inferior Temporal Gyrus	-0.27***				0.14				0.83**
			Transverse Temporal Cortex	0.25**	-0.27**	-0.42***						-0.31**
			Banks of Superior Temporal Sulcus	0.32*		-0.21	-0.01	0.9***				
INSULAR LOBULE			Insular Cortex	-0.46***	0.16	-0.29**		-0.1			0.53***	
FRONTAL LOBE	DORSO-LATERAL PFC	SUPERIOR	Superior Frontal Gyrus	-0.04		0.46***	-0.35***				-0.12	
		MIDDLE	Caudal Middle Frontal Gyrus	0.22*		0.34***				-0.11		
			Rostral Middle Frontal Gyrus	-0.18	0.8***		-0.49***			-0.08		
	VENTRO-LATERAL PFC	INFERIOR FRONTAL GYRUS	Pars Opercularis	0.04	0.28*		-0.64***					
			Pars Triangularis	-0.08	0.45***		-0.33***					
			Pars Orbitalis	-0.32**	0.58***							
	VENTROMEDIAL PREFRONTAL CORTEX		Lateral Orbitofrontal Cortex	-0.62***	0.4***			-0.19*				
			Medial Orbitofrontal Cortex	-0.7***	0.51***				-0.41***	0.09		
			Frontal Pole	-0.35**	0.56			-0.12			0.1	
	PRIMARY SENSORIMOTOR REGIONS		Precentral Gyrus	0.32***	-0.51***				-0.24**			
			Paracentral Gyrus	0.36***	-0.5***				-0.18			
PARIETAL			Postcentral Gyrus	0.49***	-0.03	-0.18**						
	SUPERIOR PARIETAL LOBULE		Superior Parietal Cortex	0.72***		0.35***	0.3**	-0.23*		0		
			Precuneus	0.41***		0.35***	0.12					
	INFERIOR PARIETAL LOBULE		Inferior Parietal Cortex	0.38***		0.24*	0.63***	0.33**				
			Supramarginal Gyrus	0.4***			0.47***	0.47***			0.59***	
CINGULATE GYRUS			Rostral Anterior Cingulate Cortex	-0.64***	0.19*		0.06		-0.22*	0.24**		
			Caudal Anterior Cingulate Cortex	-0.48***						0.48***		
			Posterior Cingulate Cortex	-0.25						0.91***		
			Isthmus of Cingulate Gyrus	-0.11				0.12		0.56***		
OCCIPITAL LOBE			Lateral Occipital Cortex	0.16					0.64***			
			Cuneus	0.01					0.63***			
			Lingual Gyrus	-0.09					0.56***			
			Pericalcarine Cortex	0.07			0.37**		0.67***			-0.23

Note. Table presents confirmatory factor analysis results for 34 brain regions specified based on the bifactor structure with eight specific factors. Standardized estimates of factor loadings are shown and were produced by estimating the model using the genetic correlation matrix as input. Negative loadings are depicted in red and positive in blue, intensity of color reflects magnitude. GEN = general factor, FAC = factor. [* for $p \leq 0.05$; ** for $p \leq 0.01$; *** for $p \leq 0.001$]

Figure 1

Relationship Between Genetic Correlations, Anatomical Distance, and Functional Boundaries

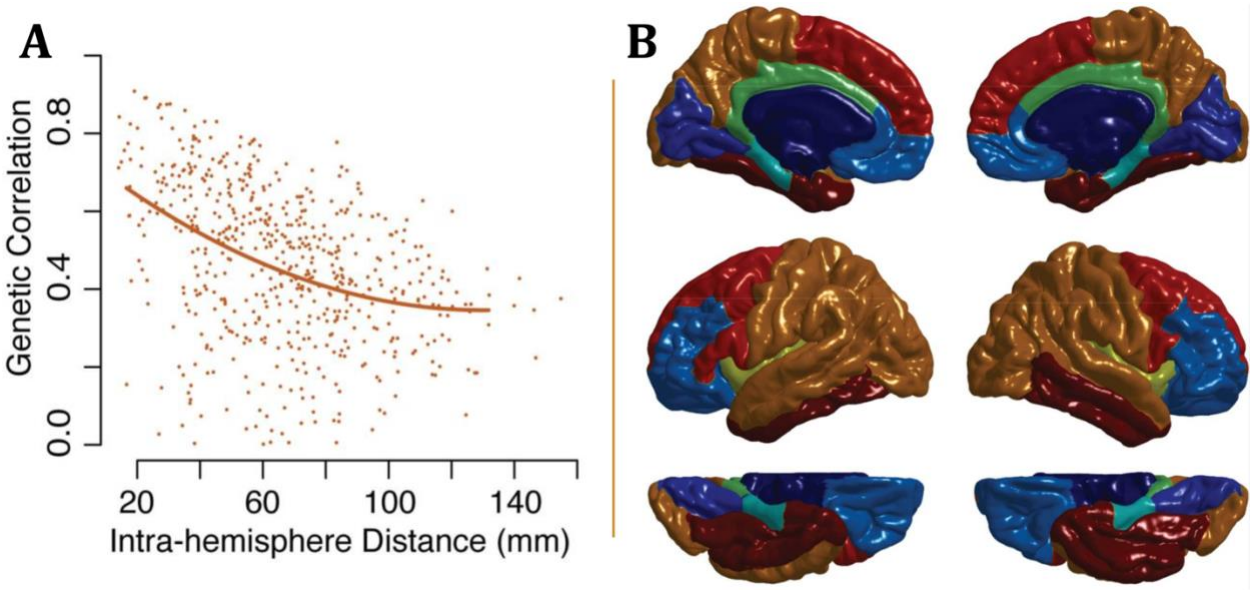

Note. (A) Fit of a quadratic polynomial model to the relationship between genetic correlations between measures of regional cortical thickness and anatomical distance within hemispheres. A quadratic model fit better than a linear model, a cubic model, and an exponential decay model. (B) Illustration of the partition (modular community structure) with 8 cortical modules, each shown in a different color, found by Alexander-Bloch et al. (2019). Medial occipital regions are in purple, dorsolateral prefrontal regions in red, ventromedial prefrontal regions in blue, and limbic regions in green. Adapted from "Human cortical thickness organized into genetically-determined communities across spatial resolutions," by A.F. Alexander-Bloch et al., 2019, *Cerebral Cortex*, *29*(1), p. 106-118.

Figure 2

Heatmap of Genetic Correlations

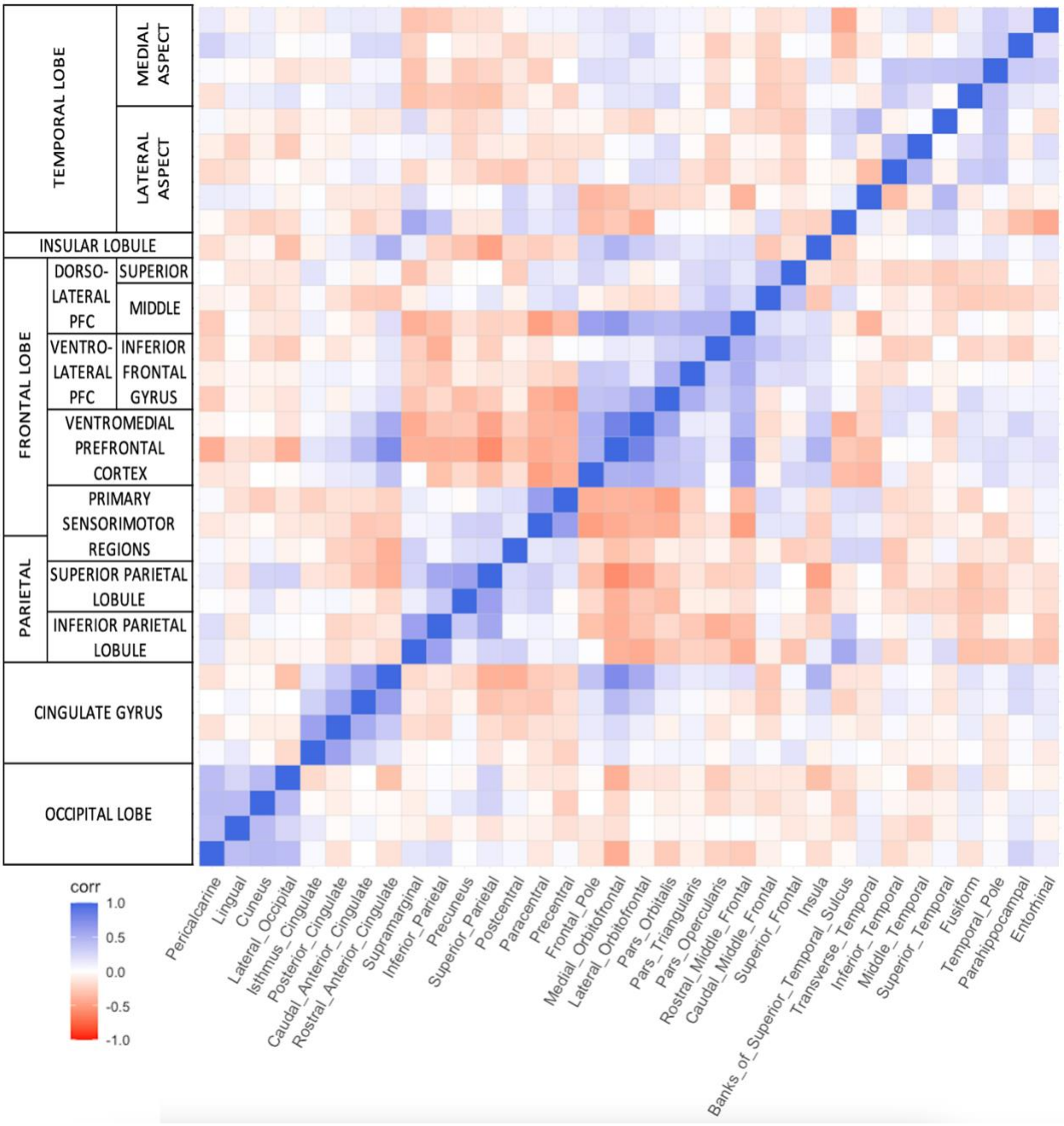

Note. Genetic heatmap estimated using LD-score regression. All pair-wise correlations between thickness measures in 34 brain regions are shown with color scale indicating the strength of the genetic correlation. Names of regions are shown to the bottom of the heat map.

Figure 3

Types of Confirmatory Models Tested

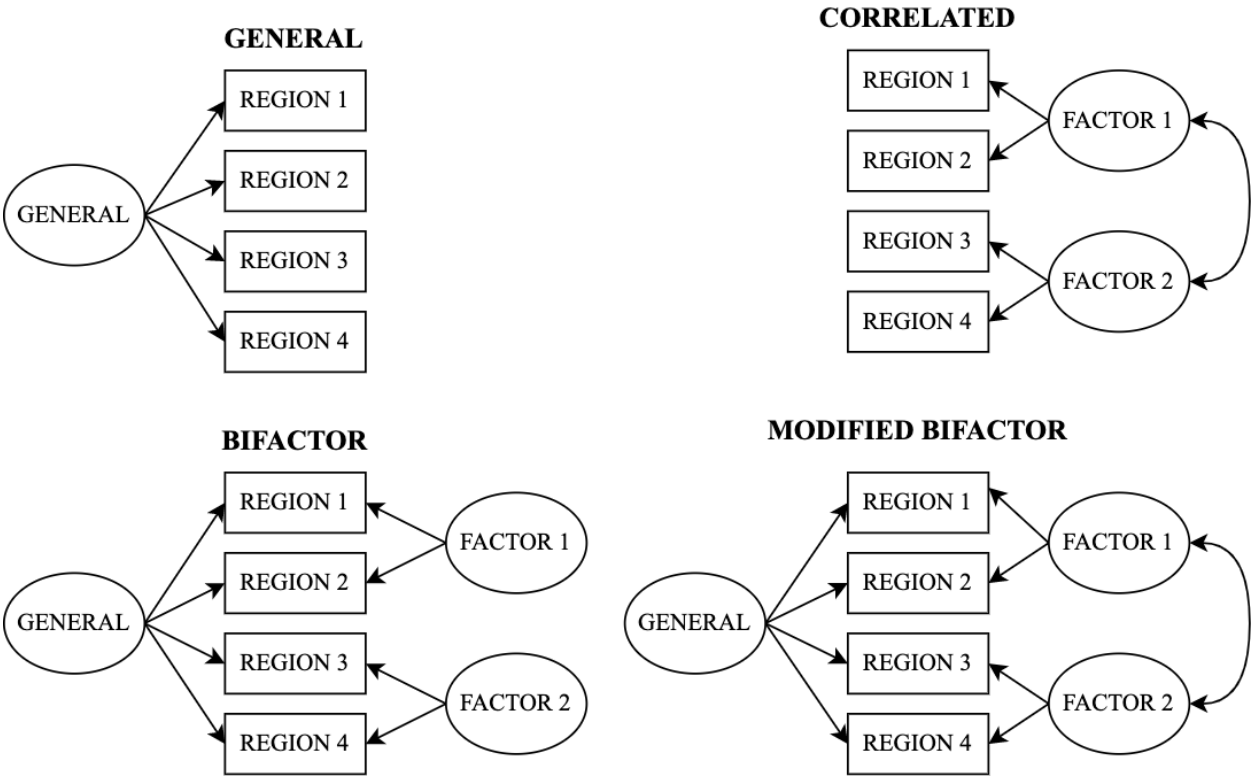

Note. Four models were tested for each of the factor solutions derived from EFAs, examples of each type of confirmatory model are illustrated using path diagrams. Indicator (observed) variables are represented by blue rectangles, latent variables by red circles, factor loadings with single-headed arrows, and factor intercorrelations by double-headed arrows. Upper left panel depicts a single, common factor model. Upper right panel depicts a correlated factors model; an orthogonal factors model has the same structure but without factor intercorrelations. Bottom left panel depicts a bifactor model with orthogonal specific factors. Bottom right panel depicts a modified bifactor model, in other words, a bifactor model with correlated specific factors.

Figure 4

Physical Location of Eight Genomic Factors

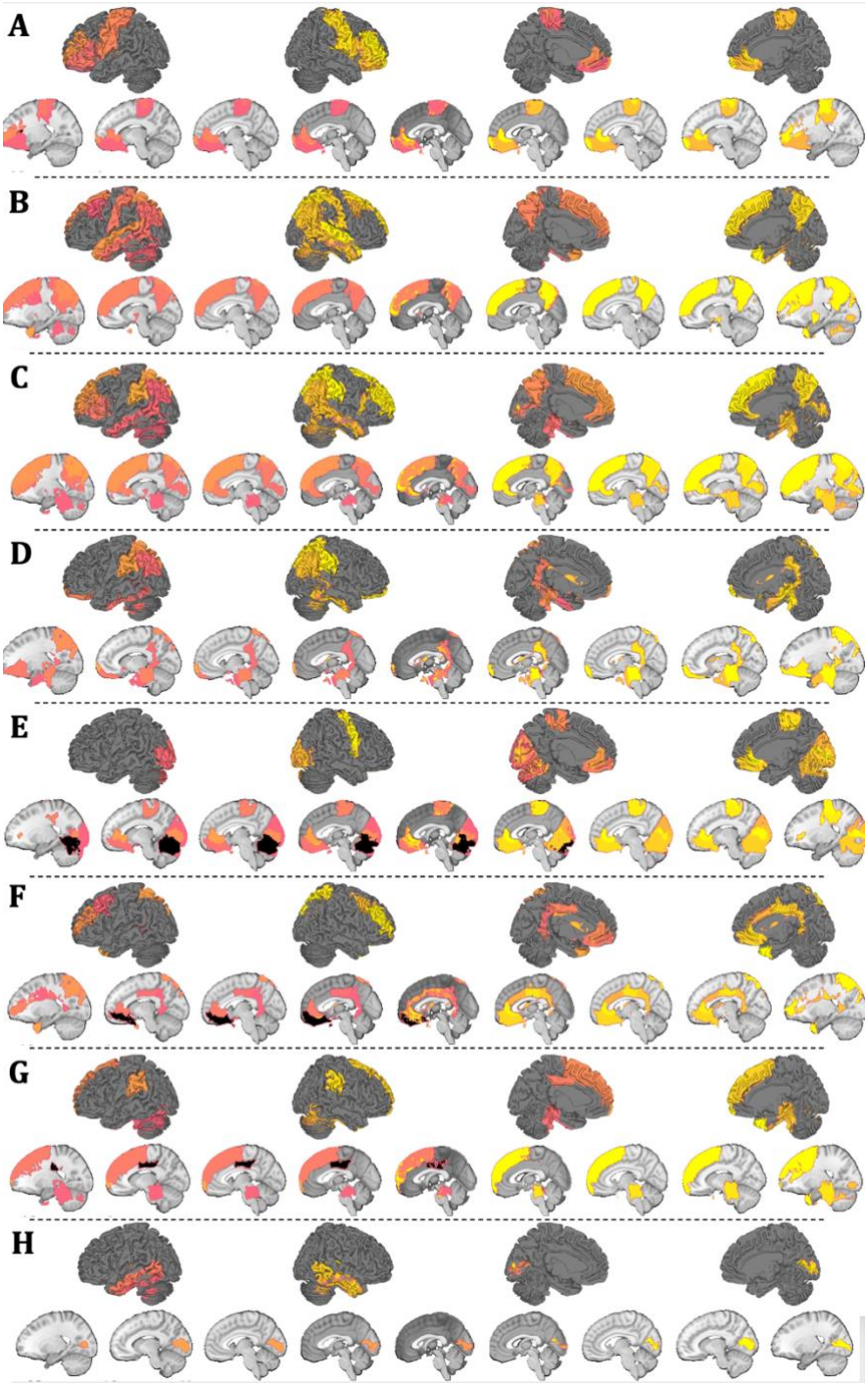

Note. Brain regions color coded according to the eight genomic factors with right hemisphere in yellow and left in pink. (A) Factor F1, (B) F2, (C) F3, (D) F4, (E) F5, (F) F6, (G) F7, (H) F8.

References

Adelstein, J. S., Shehzad, Z., Mennes, M., Deyoung, C. G., Zuo, X.-N., Kelly, C., Margulies, D. S., Bloomfield, A., Gray, J. R., Castellanos, F. X., & Milham, M. P. (2011). Personality is reflected in the brain's intrinsic functional architecture. *PloS One*, *6*(11), e27633. https://doi.org/10.1371/journal.pone.0027633

Alexander-Bloch, A. F., Mathias, S. R., Fox, P. T., Olvera, R. L., Göring, H. H. H., Duggirala, R., Curran, J. E., Blangero, J., & Glahn, D. C. (2019). Human cortical thickness organized into genetically-determined communities across spatial resolutions. *Cerebral Cortex*, *29*(1), 106–118. https://doi.org/10.1093/cercor/bhx309

Alexander-Bloch, A. F., Reiss, P. T., Rapoport, J., McAdams, H., Giedd, J. N., Bullmore, E. T., & Gogtay, N. (2014). Abnormal cortical growth in schizophrenia targets normative modules of synchronized development. *Biological Psychiatry*, *76*(6), 438–446. https://doi.org/10.1016/j.biopsych.2014.02.010

Allen, T., & Deyoung, C. (2016). Personality neuroscience and the Five-Factor Model. In T. A. Widiger (Ed.), *The Oxford Handbook of the Five Factor Model of Personality* (pp. 319–349). Oxford University Press. https://doi.org/10.1093/oxfordhb/9780199352487.013.26

Almeida Montes, L. G., Prado Alcántara, H., Martínez García, R. B., De La Torre, L. B., Ávila Acosta, D., & Duarte, M. G. (2013). Brain cortical thickness in ADHD: Age, sex, and clinical correlations. *Journal of Attention Disorders*, *17*(8), 641–654. https://doi.org/10.1177/1087054711434351

Amunts, K., Lepage, C., Borgeat, L., Mohlberg, H., Dickscheid, T., Rousseau, M.-É., Bludau, S., Bazin, P.-L., Lewis, L. B., Oros-Peusquens, A.-M., Shah, N. J., Lippert, T., Zilles, K., &

Evans, A. C. (2013). BigBrain: An ultrahigh-resolution 3D human brain model. *Science*, *340*(6139), 1472–1475. https://doi.org/10.1126/science.1235381

Aschard, H., Vilhjálmsson, B. J., Joshi, A. D., Price, A. L., & Kraft, P. (2015). Adjusting for heritable covariates can bias effect estimates in genome-wide association studies. *American Journal of Human Genetics*, *96*(2), 329–339. https://doi.org/10.1016/j.ajhg.2014.12.021

Auton, A., Abecasis, G. R., Altshuler, D. M., Durbin, R. M., Abecasis, G. R., Bentley, D. R., Chakravarti, A., Clark, A. G., Donnelly, P., Eichler, E. E., Flicek, P., Gabriel, S. B., Gibbs, R. A., Green, E. D., Hurles, M. E., Knoppers, B. M., Korbel, J. O., Lander, E. S., Lee, C., … Gravel, S. (2015). A global reference for human genetic variation. *Nature*, *526*(7571), 68–74. https://doi.org/10.1038/nature15393

Barrett, P. (2007). Structural equation modelling: Adjudging model fit. *Personality and Individual Differences*, *42*(5), 815–824. https://doi.org/10.1016/j.paid.2006.09.018

Bas-Hoogendam, J. M., van Steenbergen, H., Tissier, R. L. M., Houwing-Duistermaat, J. J., Westenberg, P. M., & van der Wee, N. J. A. (2018). Subcortical brain volumes, cortical thickness and cortical surface area in families genetically enriched for social anxiety disorder – A multiplex multigenerational neuroimaging study. *EBioMedicine*, *36*, 410–428. https://doi.org/10.1016/j.ebiom.2018.08.048

Beaujean, A. (2013). Factor analysis using R. *Practical Assessment, Research, and Evaluation*, *18*(1). https://doi.org/10.7275/z8wr-4j42

Bogdan, R., Salmeron, B. J., Carey, C. E., Agrawal, A., Calhoun, V. D., Garavan, H., Hariri, A. R., Heinz, A., Hill, M. N., Holmes, A., Kalin, N. H., & Goldman, D. (2017). Imaging

Genetics and Genomics in Psychiatry: A Critical Review of Progress and Potential. *Biological Psychiatry*, *82*(3), 165–175. https://doi.org/10.1016/j.biopsych.2016.12.030

Bulik-Sullivan, B., Finucane, H. K., Anttila, V., Gusev, A., Day, F. R., Loh, P.-R., Duncan, L., Perry, J. R. B., Patterson, N., Robinson, E. B., Daly, M. J., Price, A. L., & Neale, B. M. (2015). An atlas of genetic correlations across human diseases and traits. *Nature Genetics*, *47*(11), 1236–1241. https://doi.org/10.1038/ng.3406

Bulik-Sullivan, B. K., Loh, P.-R., Finucane, H., Ripke, S., Yang, J., Patterson, N., Daly, M. J., Price, A. L., & Neale, B. M. (2015). LD score regression distinguishes confounding from polygenicity in genome-wide association studies. *Nature Genetics*, *47*(3), 291–295. https://doi.org/10.1038/ng.3211

Bullmore, E., & Sporns, O. (2009). Complex brain networks: Graph theoretical analysis of structural and functional systems. *Nature Reviews Neuroscience*, *10*(3), 186–198. https://doi.org/10.1038/nrn2575

Campero, A., Ajler, P., Emmerich, J., Goldschmidt, E., Martins, C., & Rhoton, A. (2014). Brain sulci and gyri: A practical anatomical review. *Journal of Clinical Neuroscience*, *21*(12), 2219–2225. https://doi.org/10.1016/j.jocn.2014.02.024

Chen, C.-H., Fiecas, M., Gutiérrez, E. D., Panizzon, M. S., Eyler, L. T., Vuoksimaa, E., Thompson, W. K., Fennema-Notestine, C., Hagler, D. J., Jernigan, T. L., Neale, M. C., Franz, C. E., Lyons, M. J., Fischl, B., Tsuang, M. T., Dale, A. M., & Kremen, W. S. (2013). Genetic topography of brain morphology. *Proceedings of the National Academy of Sciences of the United States of America*, *110*(42), 17089–17094. https://doi.org/10.1073/pnas.1308091110

Chen, Z. J., He, Y., Rosa-Neto, P., Germann, J., & Evans, A. C. (2008). Revealing modular architecture of human brain structural networks by using cortical thickness from MRI. *Cerebral Cortex*, *18*(10), 2374–2381. https://doi.org/10.1093/cercor/bhn003

Coleman, J. R. I., Euesden, J., Patel, H., Folarin, A. A., Newhouse, S., & Breen, G. (2016). Quality control, imputation and analysis of genome-wide genotyping data from the Illumina HumanCoreExome microarray. *Briefings in Functional Genomics*, *15*(4), 298–304. https://doi.org/10.1093/bfgp/elv037

Desikan, R. S., Ségonne, F., Fischl, B., Quinn, B. T., Dickerson, B. C., Blacker, D., Buckner, R. L., Dale, A. M., Maguire, R. P., Hyman, B. T., Albert, M. S., & Killiany, R. J. (2006). An automated labeling system for subdividing the human cerebral cortex on MRI scans into gyral based regions of interest. *NeuroImage*, *31*(3), 968–980. https://doi.org/10.1016/j.neuroimage.2006.01.021

Eyler, L. T., Chen, C.-H., Panizzon, M. S., Fennema-Notestine, C., Neale, M. C., Jak, A., Jernigan, T. L., Fischl, B., Franz, C. E., Lyons, M. J., Grant, M., Prom-Wormley, E., Seidman, L. J., Tsuang, M. T., Fiecas, M. J. A., Dale, A. M., & Kremen, W. S. (2012). A comparison of heritability maps of cortical surface area and thickness and the influence of adjustment for whole brain measures: A magnetic resonance imaging twin study. *Twin Research and Human Genetics*, *15*(3), 304–314. https://doi.org/10.1017/thg.2012.3

Fischl, B. (2012). FreeSurfer. *NeuroImage*, *62*(2), 774–781. https://doi.org/10.1016/j.neuroimage.2012.01.021

Fischl, B., Rajendran, N., Busa, E., Augustinack, J., Hinds, O., Yeo, B. T. T., Mohlberg, H., Amunts, K., & Zilles, K. (2008). Cortical folding patterns and predicting

cytoarchitecture. *Cerebral Cortex*, *18*(8), 1973–1980. https://doi.org/10.1093/cercor/bhm225

Fouche, J.-P., du Plessis, S., Hattingh, C., Roos, A., Lochner, C., Soriano-Mas, C., Sato, J. R., Nakamae, T., Nishida, S., Kwon, J. S., Jung, W. H., Mataix-Cols, D., Hoexter, M. Q., Alonso, P., de Wit, S. J., Veltman, D. J., Stein, D. J., & van den Heuvel, O. A. (2017). Cortical thickness in obsessive-compulsive disorder: Multisite mega-analysis of 780 brain scans from six centres. *British Journal of Psychiatry*, *210*(1), 67–74. https://doi.org/10.1192/bjp.bp.115.164020

Frick, A., Howner, K., Fischer, H., Eskildsen, S. F., Kristiansson, M., & Furmark, T. (2013). Cortical thickness alterations in social anxiety disorder. *Neuroscience Letters*, *536*, 52–55. https://doi.org/10.1016/j.neulet.2012.12.060

Fuglset, T. S., Endestad, T., Hilland, E., Bang, L., Tamnes, C. K., Landrø, N. I., & Rø, Ø. (2016). Brain volumes and regional cortical thickness in young females with anorexia nervosa. *BMC Psychiatry*, *16*(1), 404. https://doi.org/10.1186/s12888-016-1126-9

Fukuchi-Shimogori, T., & Grove, E. A. (2001). Neocortex patterning by the secreted signaling molecule FGF8. *Science (New York, N.Y.)*, *294*(5544), 1071–1074. https://doi.org/10.1126/science.1064252

Gibbs, R. A., Belmont, J. W., Hardenbol, P., Willis, T. D., Yu, F., Yang, H., Ch'ang, L.-Y., Huang, W., Liu, B., Shen, Y., Tam, P. K.-H., Tsui, L.-C., Waye, M. M. Y., Wong, J. T.-F., Zeng, C., Zhang, Q., Chee, M. S., Galver, L. M., Kruglyak, S., … Tanaka, T. (2003). The international HapMap project. *Nature*, *426*(6968), 789–796. https://doi.org/10.1038/nature02168

Gold, A. L., Steuber, E. R., White, L. K., Pacheco, J., Sachs, J. F., Pagliaccio, D., Berman, E., Leibenluft, E., & Pine, D. S. (2017). cortical thickness and subcortical gray matter volume in pediatric anxiety disorders. *Neuropsychopharmacology*, *42*(12), 2423–2433. https://doi.org/10.1038/npp.2017.83

Grasby, K. L., Jahanshad, N., Painter, J. N., Colodro-Conde, L., Bralten, J., Hibar, D. P., Lind, P. A., Pizzagalli, F., Ching, C. R. K., McMahon, M. A. B., Shatokhina, N., Zsembik, L. C. P., Thomopoulos, S. I., Zhu, A. H., Strike, L. T., Agartz, I., Alhusaini, S., Almeida, M. A. A., & Aln, D. (2020). The genetic architecture of the human cerebral cortex. *Science*, *367*(6484), eaay6690. https://doi.org/10.1126/science.aay6690

Grotzinger, A. D., Mallard, T. T., Akingbuwa, W. A., Ip, H. F., Adams, M. J., Lewis, C. M., McIntosh, A. M., Grove, J., Dalsgaard, S., Lesch, K.-P., Strom, N., Meier, S. M., Mattheisen, M., Børglum, A. D., Mors, O., Breen, G., … Nivard, M. G. (2020). Genetic architecture of 11 major psychiatric disorders at biobehavioral, functional genomic, and molecular genetic levels of analysis. *Nature Genetics*, *54*, 548–559. https://doi.org/10.1101/2020.09.22.20196089

Grotzinger, A. D., Mallard, T. T., Liu, Z., Seidlitz, J., Ge, T., & Smoller, J. W. (2022). Multivariate genomic architecture of cortical thickness and surface area at multiple levels of analysis. *medRxiv*. https://doi.org/10.1101/2022.02.19.22271223

Grotzinger, A. D., Rhemtulla, M., de Vlaming, R., Ritchie, S. J., Mallard, T. T., Hill, W. D., Ip, H. F., Marioni, R. E., McIntosh, A. M., Deary, I. J., Koellinger, P. D., Harden, K. P., Nivard, M. G., & Tucker-Drob, E. M. (2019). Genomic structural equation modelling provides insights into the multivariate genetic architecture of complex traits. *Nature Human Behaviour*, *3*(5), 513–525. https://doi.org/10.1038/s41562-019-0566-x

Hanford, L. C., Nazarov, A., Hall, G. B., & Sassi, R. B. (2016). Cortical thickness in bipolar disorder: A systematic review. *Bipolar Disorders*, *18*(1), 4–18. https://doi.org/10.1111/bdi.12362

Hawrylycz, M. J., Lein, E. S., Guillozet-Bongaarts, A. L., Shen, E. H., Ng, L., Miller, J. A., van de Lagemaat, L. N., Smith, K. A., Ebbert, A., Riley, Z. L., Abajian, C., Beckmann, C. F., Bernard, A., Bertagnolli, D., Boe, A. F., Cartagena, P. M., Chakravarty, M. M., Chapin, M., Chong, J., … Jones, A. R. (2012). An anatomically comprehensive atlas of the adult human brain transcriptome. *Nature*, *489*(7416), 391–399. https://doi.org/10.1038/nature11405

Hayduk, L., Cummings, G., Boadu, K., Pazderka-Robinson, H., & Boulianne, S. (2007). Testing! Testing! One, two, three - Testing the theory in structural equation models. *Personality and Individual Differences*, *42*(5), 841–850. https://doi.org/10.1016/j.paid.2006.10.001

Hu, L., & Bentler, P. M. (1999). Cutoff criteria for fit indexes in covariance structure analysis: Conventional criteria versus new alternatives. *Structural Equation Modeling*, *6*(1), 1–55. https://doi.org/10.1080/10705519909540118

Hutzler, F. (2014). Reverse inference is not a fallacy per se: Cognitive processes can be inferred from functional imaging data. *NeuroImage*, *84*, 1061–1069. https://doi.org/10.1016/j.neuroimage.2012.12.075

Hyatt, C. J., Haney-Caron, E., & Stevens, M. C. (2012). Cortical Thickness and Folding Deficits in Conduct-Disordered Adolescents. *Biological Psychiatry*, *72*(3), 207–214. https://doi.org/10.1016/j.biopsych.2011.11.017

Jiang, W., Li, G., Liu, H., Shi, F., Wang, T., Shen, C., Shen, H., Hu, D., Wang, W., & Shen, D. (2016). Reduced cortical thickness and increased surface area in antisocial personality

disorder. *Neuroscience*, *337*, 143–152. https://doi.org/10.1016/j.neuroscience.2016.08.052

Keshavan, M., Lizano, P., & Prasad, K. (2020). The synaptic pruning hypothesis of schizophrenia: Promises and challenges. *World Psychiatry*, *19*(1), 110–111. https://doi.org/10.1002/wps.20725

Khundrakpam, B. S., Lewis, J. D., Kostopoulos, P., Carbonell, F., & Evans, A. C. (2017). Cortical thickness abnormalities in autism spectrum disorders through late childhood, adolescence, and adulthood: A large-scale MRI study. *Cerebral Cortex*, *27*(3), 1721–1731. https://doi.org/10.1093/cercor/bhx038

Kim, S., & Misra, A. (2007). SNP genotyping: Technologies and biomedical applications. *Annual Review of Biomedical Engineering*, *9*, 289–320. https://doi.org/10.1146/annurev.bioeng.9.060906.152037

Kirk, R. (2012). Experimental design. In I. Weiner, J. Schinka, & W. Velicer (Eds.), *Handbook of Psychology: Vol. 2. Research Methods in Psychology* (2nd ed., pp. 3-33). Wiley.

Koenigs, M., Barbey, A. K., Postle, B. R., & Grafman, J. (2009). Superior parietal cortex is critical for the manipulation of information in working memory. *The Journal of Neuroscience*, *29*(47), 14980–14986. https://doi.org/10.1523/JNEUROSCI.3706-09.2009

Koppenhafer, S. L., Goss, K. L., Voigt, E., Croushore, E., Terry, W. W., Ostergaard, J., Gordon, P. M., & Gordon, D. J. (2022). Inhibitor of DNA binding 2 (ID2) regulates the expression of developmental genes and tumorigenesis in ewing sarcoma. *Oncogene*, *41*(20), 2873–2884. https://doi.org/10.1038/s41388-022-02310-0

Larivière, S., Paquola, C., Park, B.-Y., Royer, J., Wang, Y., Benkarim, O., Vos de Wael, R., Valk, S. L., Thomopoulos, S. I., Kirschner, M., Lewis, L. B., Evans, A. C., Sisodiya, S.

M., McDonald, C. R., Thompson, P. M., & Bernhardt, B. C. (2021). The ENIGMA toolbox: Multiscale neural contextualization of multisite neuroimaging datasets. *Nature Methods*, *18*(7), 698–700. https://doi.org/10.1038/s41592-021-01186-4

Lavagnino, L., Mwangi, B., Cao, B., Shott, M. E., Soares, J. C., & Frank, G. K. W. (2018). Cortical thickness patterns as state biomarker of anorexia nervosa. *International Journal of Eating Disorders*, *51*(3), 241–249. https://doi.org/10.1002/eat.22828

Lee, J. J., McGue, M., Iacono, W. G., & Chow, C. C. (2018). The accuracy of LD Score regression as an estimator of confounding and genetic correlations in genome-wide association studies. *Genetic Epidemiology*, *42*(8), 783–795. https://doi.org/10.1002/gepi.22161

Lee, P. H., Anttila, V., Won, H., Feng, Y.-C. A., Rosenthal, J., Zhu, Z., Tucker-Drob, E. M., Nivard, M. G., Grotzinger, A. D., Posthuma, D., Wang, M. M.-J., Yu, D., Stahl, E. A., Walters, R. K., Anney, R. J. L., Duncan, L. E., Ge, T., Adolfsson, R., Banaschewski, T., … Smoller, J. W. (2019). Genomic relationships, novel loci, and pleiotropic mechanisms across eight psychiatric disorders. *Cell*, *179*(7), 1469-1482.e11. https://doi.org/10.1016/j.cell.2019.11.020

Li, Q., Zhao, Y., Chen, Z., Long, J., Dai, J., Huang, X., Lui, S., Radua, J., Vieta, E., Kemp, G. J., Sweeney, J. A., Li, F., & Gong, Q. (2020). Meta-analysis of cortical thickness abnormalities in medication-free patients with major depressive disorder. *Neuropsychopharmacology*, *45*(4), 703–712. https://doi.org/10.1038/s41386-019-0563-9

Lin, P., Hartz, S. M., Zhang, Z., Saccone, S. F., Wang, J., Tischfield, J. A., Edenberg, H. J., Kramer, J. R., M.Goate, A., Bierut, L. J., Rice, J. P. (2010). A new statistic to evaluate

imputation reliability. *PloS One*, *5*(3), e9697. https://doi.org/10.1371/journal.pone.0009697

Loehlin, J. C., & Beaujean, A. A. (2017). *Latent Variable Models: An Introduction to Factor, Path, and Structural Equation Analysis, Fifth Edition* (5th ed.). Routledge. https://doi.org/10.4324/9781315643199

Makris, N., Kennedy, D. N., McInerney, S., Sorensen, A. G., Wang, R., Caviness, V. S., & Pandya, D. N. (2005). Segmentation of subcomponents within the superior longitudinal fascicle in humans: A quantitative, in vivo, DT-MRI study. *Cerebral Cortex*, *15*(6), 854–869. https://doi.org/10.1093/cercor/bhh186

Makris, N., Papadimitriou, G. M., Sorg, S., Kennedy, D. N., Caviness, V. S., & Pandya, D. N. (2007). The occipitofrontal fascicle in humans: A quantitative, in vivo, DT-MRI study. *NeuroImage*, *37*(4), 1100–1111. https://doi.org/10.1016/j.neuroimage.2007.05.042

Markon, K. E. (2019). Bifactor and hierarchical models: Specification, inference, and interpretation. *Annual Review of Clinical Psychology*, *15*(1), 51-69. https://doi.org/10.1146/annurev-clinpsy-050718-095522

Miller, G. A., & Rockstroh, B. (2013). Endophenotypes in psychopathology research: Where do we stand? *Annual Review of Clinical Psychology*, *9*, 177–213. https://doi.org/10.1146/annurev-clinpsy-050212-185540

Molent, C., Maggioni, E., Cecchetto, F., Garzitto, M., Piccin, S., Bonivento, C., Maieron, M., D'Agostini, S., Balestrieri, M., Perna, G., Altamura, A. C., & Brambilla, P. (2018). Reduced cortical thickness and increased gyrification in generalized anxiety disorder: A 3 T MRI study. *Psychological Medicine*, *48*(12), 2001–2010. https://doi.org/10.1017/S003329171700352X

O'Leary, D. D. M., Chou, S.-J., & Sahara, S. (2007). Area patterning of the mammalian cortex. *Neuron*, *56*(2), 252–269. https://doi.org/10.1016/j.neuron.2007.10.010

Ozer, D. J., & Benet-Martínez, V. (2006). Personality and the prediction of consequential outcomes. *Annual Review of Psychology*, *57*, 401–421. https://doi.org/10.1146/annurev.psych.57.102904.190127

Poldrack, R. A. (2011). Inferring mental states from neuroimaging data: From reverse inference to large-scale decoding. *Neuron*, *72*(5), 692–697. https://doi.org/10.1016/j.neuron.2011.11.001

Poldrack, R. A., & Gorgolewski, K. J. (2017). OpenfMRI: Open sharing of task fMRI data. *NeuroImage*, *144*, 259–261. https://doi.org/10.1016/j.neuroimage.2015.05.073

Poldrack, R., Kittur, A., Kalar, D., Miller, E., Seppa, C., Gil, Y., Parker, D., Sabb, F., & Bilder, R. (2011). The Cognitive Atlas: Toward a knowledge foundation for cognitive neuroscience. *Frontiers in Neuroinformatics*, *5*. https://www.frontiersin.org/article/10.3389/fninf.2011.00017

Rakic, P. (2009). Evolution of the neocortex: A perspective from developmental biology. *Nature Reviews Neuroscience*, *10*(10), 724–735. https://doi.org/10.1038/nrn2719

Rasetti, R., & Weinberger, D. R. (2011). Intermediate phenotypes in psychiatric disorders. *Current Opinion in Genetics & Development*, *21*(3), 340–348. https://doi.org/10.1016/j.gde.2011.02.003

Rimol, L. M., Panizzon, M. S., Fennema-Notestine, C., Eyler, L. T., Fischl, B., Franz, C. E., Hagler, D. J., Lyons, M. J., Neale, M. C., Pacheco, J., Perry, M. E., Schmitt, J. E., Grant, M. D., Seidman, L. J., Thermenos, H. W., Tsuang, M. T., Eisen, S. A., Kremen, W. S., & Dale, A. M. (2010). Cortical thickness is influenced by regionally specific genetic

factors. *Biological Psychiatry*, *67*(5), 493–499. https://doi.org/10.1016/j.biopsych.2009.09.032

Rolls, E. T. (2004). The functions of the orbitofrontal cortex. *Brain and Cognition*, *55*(1), 11–29. https://doi.org/10.1016/S0278-2626(03)00277-X

Russell, D. W. (2002). In search of underlying dimensions: The use (and abuse) of factor analysis in personality and social psychology. *Personality and Social Psychology Bulletin*, *28*(12), 1629–1646. https://doi.org/10.1177/014616702237645

Schmitt, J. E., Wallace, G. L., Lenroot, R. K., Ordaz, S. E., Greenstein, D., Clasen, L., Kendler, K. S., Neale, M. C., & Giedd, J. N. (2010). A twin study of intracerebral volumetric relationships. *Behavior Genetics*, *40*(2), 114–124. https://doi.org/10.1007/s10519-010-9332-6

Schmitt, J. E., Wallace, G. L., Rosenthal, M. A., Molloy, E. A., Ordaz, S., Lenroot, R., Clasen, L. S., Blumenthal, J. D., Kendler, K. S., Neale, M. C., & Giedd, J. N. (2007). A multivariate analysis of neuroanatomic relationships in a genetically informative pediatric sample. *NeuroImage*, *35*(1), 70–82. https://doi.org/10.1016/j.neuroimage.2006.04.232

Shaw, P., Kabani, N. J., Lerch, J. P., Eckstrand, K., Lenroot, R., Gogtay, N., Greenstein, D., Clasen, L., Evans, A., Rapoport, J. L., Giedd, J. N., & Wise, S. P. (2008). Neurodevelopmental trajectories of the human cerebral cortex. *Journal of Neuroscience*, *28*(14), 3586–3594. https://doi.org/10.1523/JNEUROSCI.5309-07.2008

Smoller, J. W., Andreassen, O. A., Edenberg, H. J., Faraone, S. V., Glatt, S. J., & Kendler, K. S. (2019). Psychiatric genetics and the structure of psychopathology. *Molecular Psychiatry*, *24*(3), 409–420. https://doi.org/10.1038/s41380-017-0010-4

Song, L., Zhou, Z., Meng, J., Zhu, X., Wang, K., Wei, D., & Qiu, J. (2021). Rostral middle frontal gyrus thickness mediates the relationship between genetic risk and neuroticism trait. *Psychophysiology*, *58*(2), e13728. https://doi.org/10.1111/psyp.13728

Spocter, M. A., Hopkins, W. D., Barks, S. K., Bianchi, S., Hehmeyer, A. E., Anderson, S. M., Stimpson, C. D., Fobbs, A. J., Hof, P. R., & Sherwood, C. C. (2012). Neuropil distribution in the cerebral cortex differs between humans and chimpanzees. *The Journal of Comparative Neurology*, *520*(13), 2917–2929. https://doi.org/10.1002/cne.23074

Thompson, P., Jahanshad, N., Ching, C. R. K., Salminen, L., Thomopoulos, S. I., Bright, J., Baune, B. T., Bertolín, S., Bralten, J., Bruin, W. B., Bülow, R., Chen, J., Chye, Y., Dannlowski, U., de Kovel, C. G. F., Donohoe, G., Eyler, L., Faraone, S. V., Favre, P., … Zelman, V. (2020). ENIGMA and global neuroscience: A decade of large-scale studies of the brain in health and disease across more than 40 countries. *Translational Psychiatry*, *10*(1), 100. https://doi.org/10.1038/s41398-020-0705-1

Triarhou, L. C. (2007). The Economo-Koskinas atlas revisited: Cytoarchitectonics and functional context. *Stereotactic and Functional Neurosurgery*, *85*(5), 195–203. https://doi.org/10.1159/000103258

Tzourio-Mazoyer, N., Zago, L., Cochet, H., & Crivello, F. (2020). Development of handedness, anatomical and functional brain lateralization. In A. Gallagher, C. Bulteau, D. Cohen, & J. L. Michaud (Eds.), *Handbook of Clinical Neurology* (Vol. 173, pp. 99–105). Elsevier. https://doi.org/10.1016/B978-0-444-64150-2.00011-3

Valk, S. L., Hoffstaedter, F., Camilleri, J. A., Kochunov, P., Yeo, B. T. T., & Eickhoff, S. B. (2020). Personality and local brain structure: Their shared genetic basis and

reproducibility. *NeuroImage*, *220*(117067). https://doi.org/10.1016/j.neuroimage.2020.117067

Van Essen, D. C., & Glasser, M. F. (2016). The Human Connectome Project: Progress and Prospects. *Cerebrum: The Dana Forum on Brain Science*, *2016*, cer-10-16.

Vanderhaeghen, P., & Cheng, H.-J. (2010). Guidance molecules in axon pruning and cell death. *Cold Spring Harbor Perspectives in Biology*, *2*(6), a001859. https://doi.org/10.1101/cshperspect.a001859

Vértes, P. E., Alexander-Bloch, A. F., Gogtay, N., Giedd, J. N., Rapoport, J. L., & Bullmore, E. T. (2012). Simple models of human brain functional networks. *Proceedings of the National Academy of Sciences of the United States of America*, *109*(15), 5868–5873. https://doi.org/10.1073/pnas.1111738109

von Economo, C., & Koskinas, G. (1926). Die cytoarchitektonik der hirnrinde des erwachsenen menschen. *Archives of Neurology and Psychiatry*, *16*(6), 816.

Waldman I.D. et al. (2022). Recommendations for adjudicating among alternative structural models of psychopathology. *psyArxiv*.

Winkler, A. M., Kochunov, P., Blangero, J., Almasy, L., Zilles, K., Fox, P. T., Duggirala, R., & Glahn, D. C. (2010). Cortical thickness or grey matter volume? The importance of selecting the phenotype for imaging genetics studies. *NeuroImage*, *53*(3), 1135–1146. https://doi.org/10.1016/j.neuroimage.2009.12.028

Wrocklage, K. M., Averill, L. A., Scott, J. C., Averill, C. L., Schweinsburg, B., Trejo, M., Roy, A., Weisser, V., Kelly, C., Martini, B., Harpaz-Rotem, I., Southwick, S. M., Krystal, J. H., & Abdallah, C. G. (2017). Cortical thickness reduction in combat exposed U.S.

veterans with and without PTSD. *European Neuropsychopharmacology*, *27*(5), 515–525. https://doi.org/10.1016/j.euroneuro.2017.02.010

Yan, J., Cui, Y., Li, Q., Tian, L., Liu, B., Jiang, T., Zhang, D., & Yan, H. (2019). Cortical thinning and flattening in schizophrenia and their unaffected parents. *Neuropsychiatric Disease and Treatment*, *15*, 935–946. https://doi.org/10.2147/NDT.S195134

Yarkoni, T. (2015). Neurobiological substrates of personality: A critical overview. In *APA Handbook of Personality and Social Psychology, Volume 4: Personality Processes and Individual Differences* (pp. 61–83). American Psychological Association. https://doi.org/10.1037/14343-003

Yeo, T., Krienen, F. M., Sepulcre, J., Sabuncu, M. R., Lashkari, D., Hollinshead, M., Roffman, J. L., Smoller, J. W., Zöllei, L., Polimeni, J. R., Fischl, B., Liu, H., & Buckner, R. L. (2011). The organization of the human cerebral cortex estimated by intrinsic functional connectivity. *Journal of Neurophysiology*, *106*(3), 1125–1165. https://doi.org/10.1152/jn.00338.2011

Zwick, W. R., & Velicer, W. F. (1982). Factors influencing four rules for determining the number of components to retain. *Multivariate Behavioral Research*, *17*(2), 253–269. https://doi.org/10.1207/s15327906mbr1702_5